Tides and Numerical Modelling of Tides

Jithin Abraham K
Project Scientist B
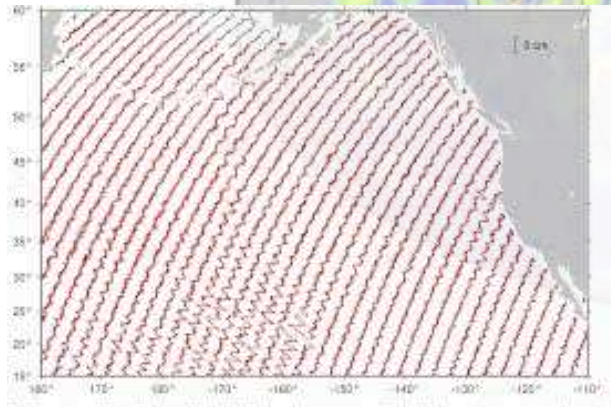**Modelling and Data Assimilation DIvision (MDA)**
Indian National Centre for Ocean Information Services (INCOIS)

Training course on "Fundamentals of Ocean Modelling"
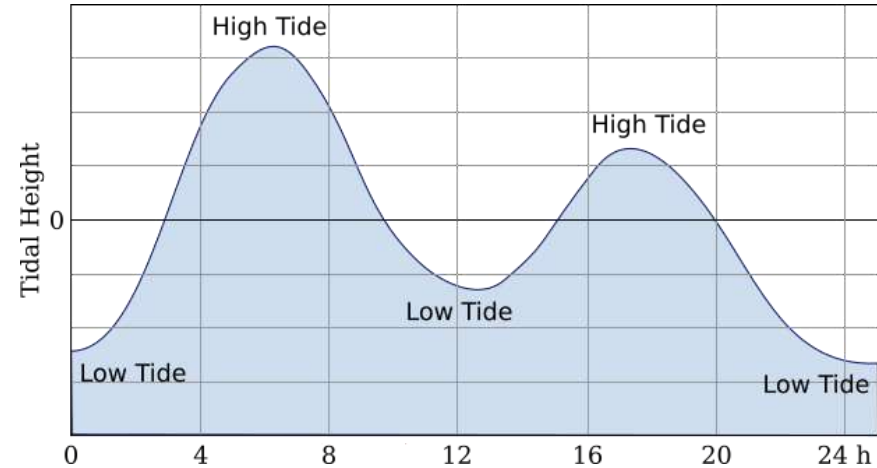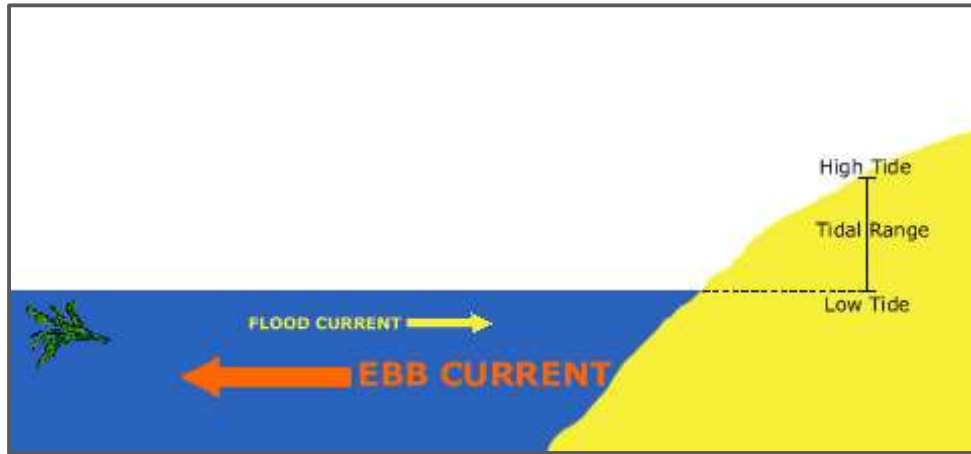**27 September - 1 October, 2021**
International Training Centre for Operational Oceanography (ITCOocean)
ESSO-INCOIS, Hyderabad, India

Barotropic tides in the Ocean

Tides are the periodic rise and fall of the ocean surface, which are generated as the response of the gravitational body force exerted by the Moon and Sun and the rotation of the Earth-Moon-Sun system.

Nature of tidal oscillations

An area has a semidiurnal tidal cycle if it experiences two high and two low tides of approximately equal size every lunar day.

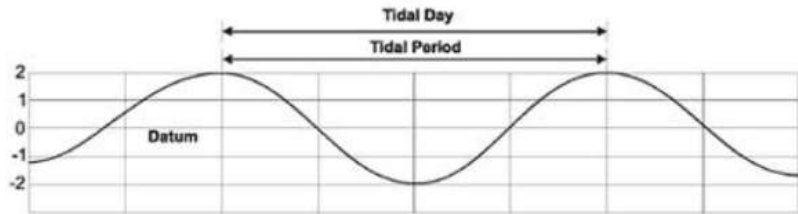An area has a diurnal tidal cycle if it experiences one high and one low tide every lunar day.

A mixed tide is a tidal cycle which consists of two unequal high tides and two unequal low tides in approximately a 24 hour period.
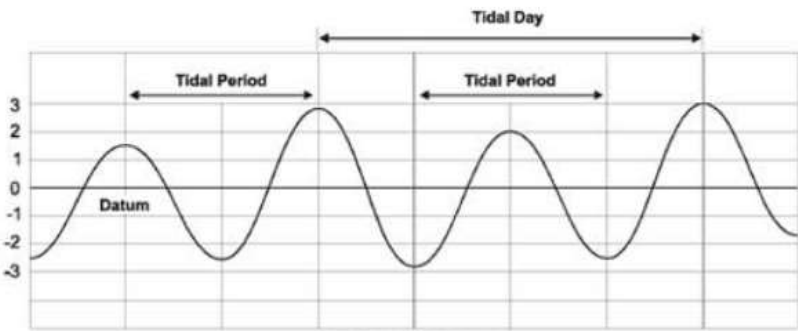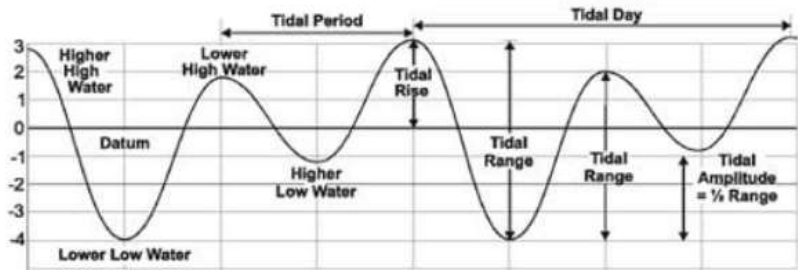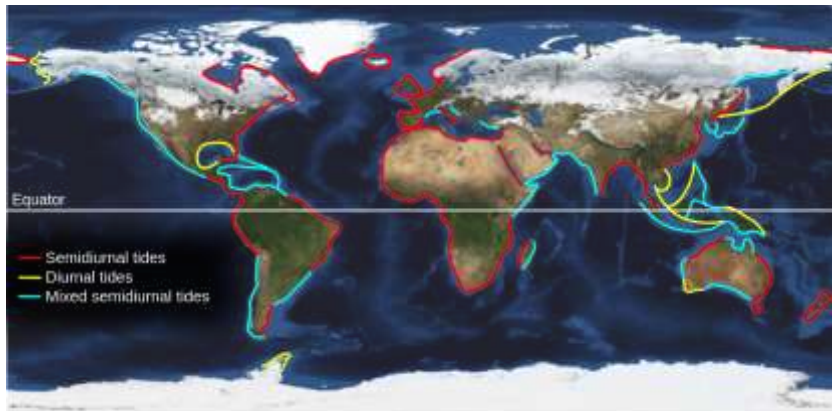
Tide generating forces
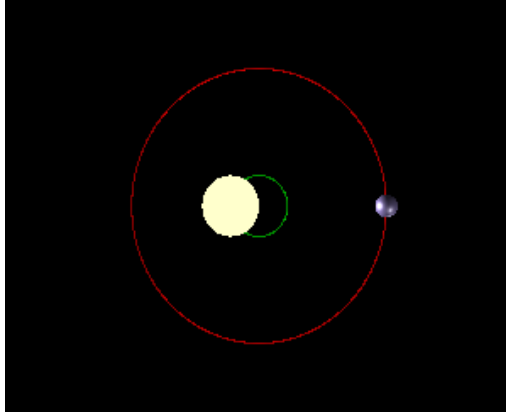

- **Gravitational attraction of moon and sun.**
- **The rotation of earth-moon system.**

The moon doesn't just orbit the Earth—both the Earth and the Moon orbit around their barycenter (G). E1, E2, and E3 indicate the position of the Earth's center of mass at different times during the orbit. The corresponding points M1, M2 and M3 indicate the position of the Moon's center of mass at these same times, respectively. The distance from the earth to the moon is not to scale.

centrifugal force
gravitational force due to Moon
tide-producing force

Barycentre, due to the difference of the mass of earth and moon, is located approximately 3/4 of the earth's radius from the earth center.

Tide generating force

The earth and moon are locked in the motion, rotating with the period of one month.
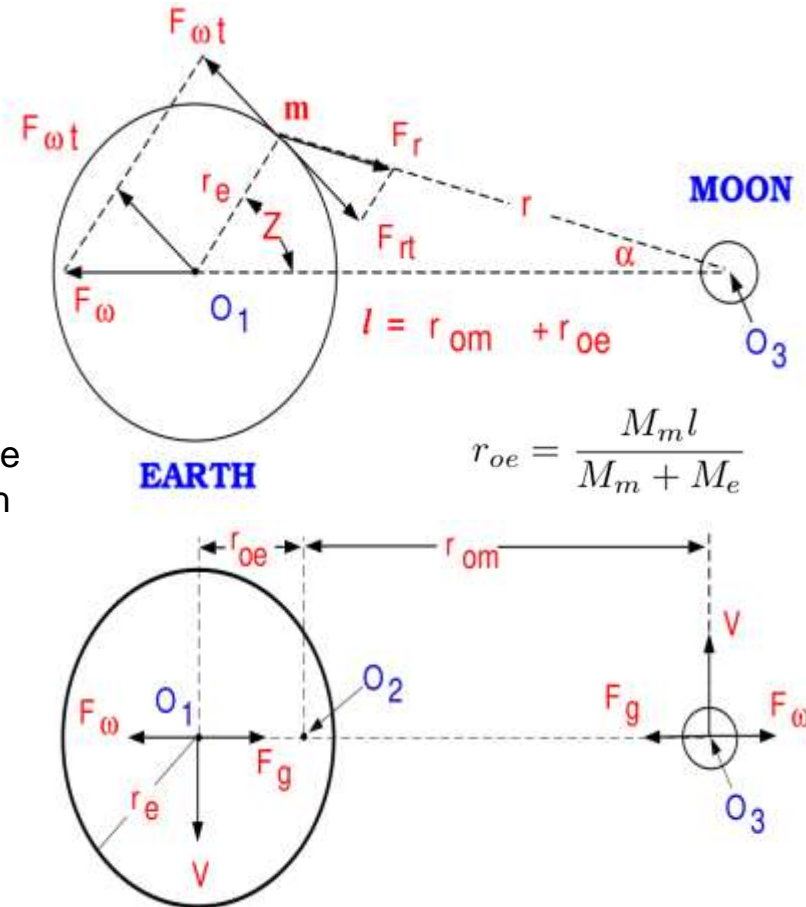**The earth-moon system is kept in the dynamical equilibrium by two forces.** One of them is the centrifugal force:

$$F_\omega = M \frac{V^2}{r_o}$$

Here M is the mass of earth or the moon, V is the velocity of the earth or moon and r_o is the radius of the orbit either of the earth ($r_o = r_{oe}$) or the orbit of the moon ($r_o = r_{om}$)

The second force (F_g) is the force of gravitational attraction. For the earth-moon system it is expressed as:
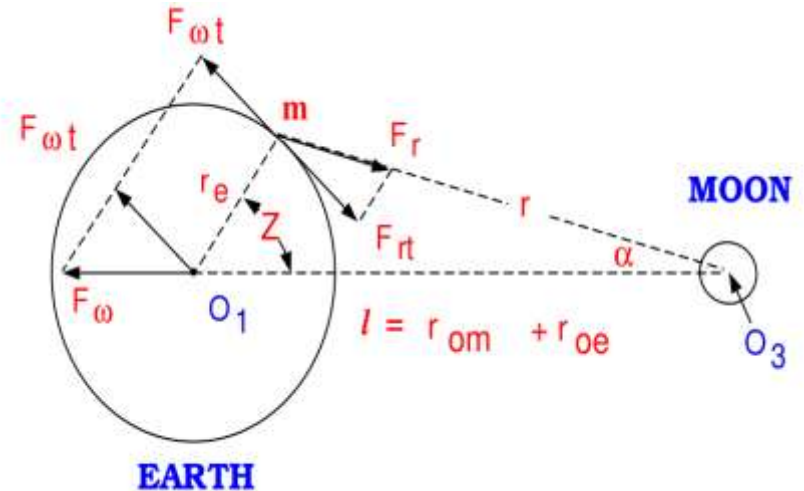
$$F_g = G \frac{M_e M_m}{l^2}$$

Reference
The Oceanography of Tides
by
Zygmunt Kowalik and John Luick

$$r_{oe} = \frac{M_m l}{M_m + M_e}$$

$$l = r_{om} + r_{oe}$$

For the system earth-moon to be in the equilibrium the vector sum of the two forces ought to be zero, both in the center of the earth and in the center of the moon. Therefore, **F$_w$** must be equal to **F$_g$**

$$\vec{F}_\omega = \vec{F}_g$$

The rotational motion around common center of gravity is somewhat different from the motion described by a wheel. Earth and moon revolves around the common center without rotation through a simple translation.

Reference
**The Oceanography of Tides**
by
Zygmunt Kowalik and John Luick

To simplify considerations and to make picture more lucid we shall move the barycentre O_2 from inside the earth to the outside. The revolution of the earth around point O_2 proceeds in such way that every particle located on earth describe a circle of the same radius $r = r_o$. Therefore, for each particle

$$(F_\omega)_A = (F_\omega)_B = (F_\omega)_{O_1} = F_g$$

Thus, every point in the revolving motion is subject to the equal and parallel centrifugal forces. Stability of the earth-moon system will require that the sum of all centrifugal and attraction forces should be zero. While this statement is true for the centers of the earth and moon the balance does not occur in every point leading to the forces generating tides.
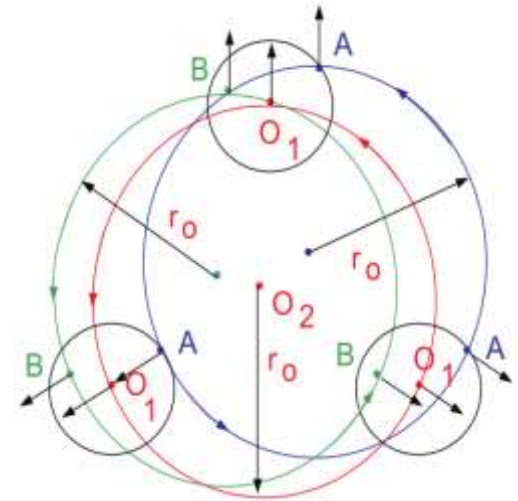
To find these forces let us consider a mass m located on the earth's surface. The centrifugal force F_ω is the same for the every point on the earth and according to Previous equation is equal to the force of attraction which moon exerts on the mass (m) located at the center of the earth;
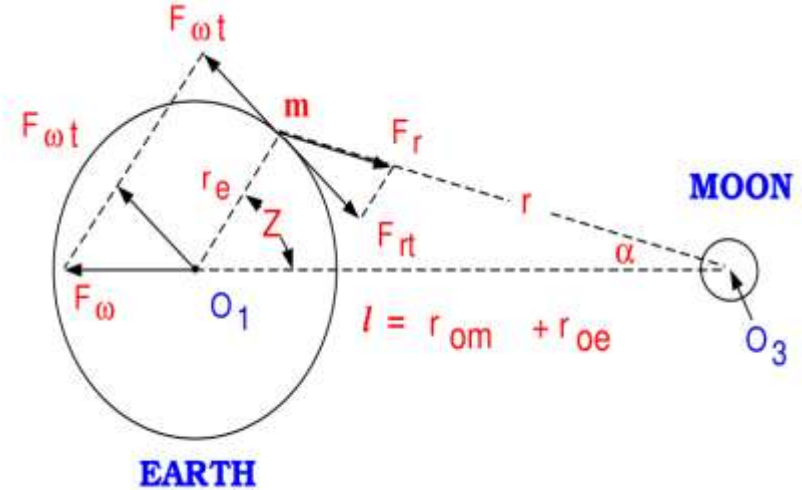
$$F_\omega = F_g = G\frac{M_m m}{l^2}$$

The force of the moon attraction acting on the mass m located on the earth's surface

$$F_r = G\frac{M_m m}{r^2}$$

Projection of these forces on the tangential direction to the earth's surface yield,

$$F_{\omega t} = G\frac{M_m m}{l^2}\sin Z$$

and

$$F_{rt} = G\frac{M_m m}{r^2}\sin(Z+\alpha)$$

Where Z is zenith angle.

Summing up these forces we arrive at the tide generating force F_t

$$F_t = GM_m m \left[\frac{\sin(Z + \alpha)}{r^2} - \frac{\sin Z}{l^2} \right]$$

From the triangle O_1, m, O_3 we can find:

$$\frac{\sin Z}{r} = \frac{\sin(\pi - Z - \alpha)}{l} = \frac{\sin(Z + \alpha)}{l}$$

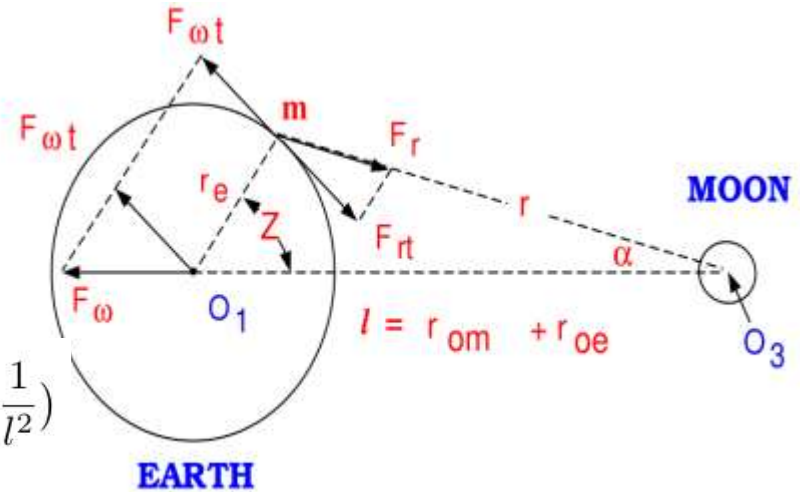Therefore sin(Z + α) can be expressed by sin Z and

$$F_t = GM_m m \left[\frac{\sin(Z + \alpha)}{r^2} - \frac{\sin Z}{l^2} \right] = GM_m m \sin Z \left(\frac{l}{r^3} - \frac{1}{l^2} \right)$$

Again using the triangle O_1 , m, O_3 the distance r is defined as:

$$r^2 = l^2 + r_e^2 - 2r_e l \cos Z$$

Since the equatorial parallax ratio for the moon r_e /l is very small number (1/60.3) and for the sun this number is even smaller

$$\frac{r_e}{l_m} = 0.01658 \qquad \frac{r_e}{l_s} = 4.2615 \times 10^{-5}$$
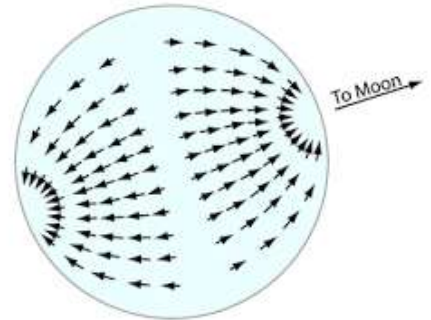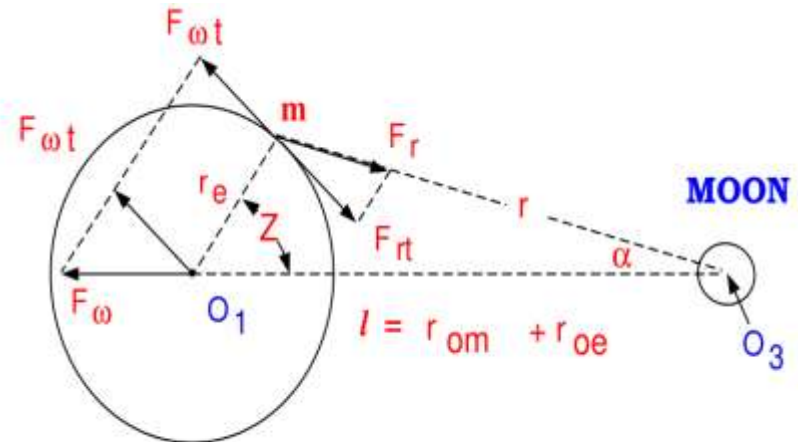
the terms of the higher order ($r_e^2/l^2 \sim 1/3600$) will be neglected. Developing above equation into binomial series we arrive at,

$$\frac{1}{r^3} \simeq \frac{1}{l^3}\left(1 + \frac{3r_e}{l}\cos Z\right)$$

Introducing this result into the **horizontal component of the tide generating force,** yields,

$$F_t = GM_m m \sin Z\left(\frac{l}{r^3} - \frac{1}{l^2}\right) = 3GM_m m \frac{r_e}{l^3}\sin Z \cos Z = \frac{3}{2}GM_m m \frac{r_e}{l^3}\sin 2Z$$

$$F_n = F_{rn} - F_{\omega n} = 3GM_m m \frac{r_e}{l^3}\left(\cos^2 Z - \frac{1}{3}\right)$$

To the tidal forces the notion of the potential (Ω) can be ascribed assuming that force per unit mass (F/m) and potential are connected as follows

$$\frac{\vec{F}}{m} = -\nabla\Omega_T$$

Reference
The Oceanography of Tides
by
Zygmunt Kowalik and John Luick

In the system of coordinate from Fig. I.5, normal direction is away from the center of the earth and tangential direction is along F_{wt} (compare also Fig I.2),

$$-F_t/m = -\frac{\partial\Omega_T}{\partial s} = -\frac{1}{r_e}\frac{\partial\Omega_T}{\partial Z} \qquad (I.34)$$

$$F_n/m = -\frac{\partial\Omega_T}{\partial n} = -\frac{\partial\Omega_T}{\partial r_e} \qquad (I.35)$$

Using eqs(I.31) and (I.32) the **potential of the tidal force** follows,

$$\Omega_T = \frac{3}{2}GM_m\frac{r_e^2}{l^3}(\frac{1}{3} - \cos^2 Z)$$

$$\Omega_T = \frac{3}{2}GM_m\frac{r_e^2}{l^3}(\frac{1}{3} - \cos^2 Z)$$

This expression is of the first approximation. It works well for the sun-earth interaction but because of the moon proximity to the earth sometimes higher order effects become important. For such case the distance in eq(I.29) can be developed to derive next term in series;

$$\Omega_T = \frac{3}{2l}GM_m\left[\frac{r_e^2}{l^2}(\frac{1}{3} - \cos^2 Z) + \frac{r_e^3}{l^3}(3 - 5\cos^2 Z)\right] \qquad (I.37)$$

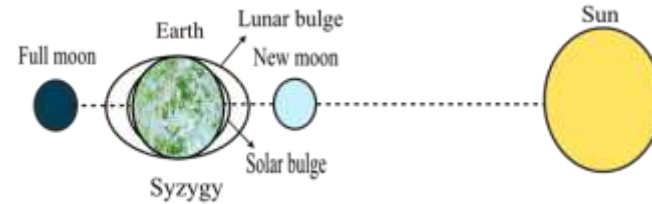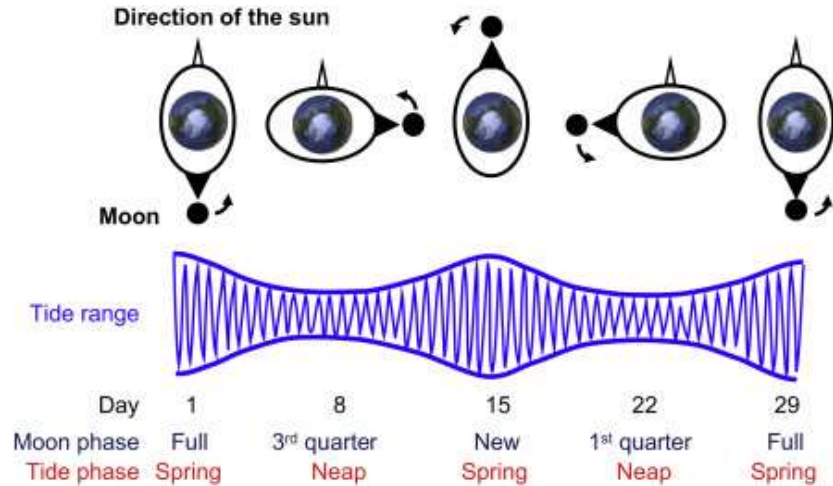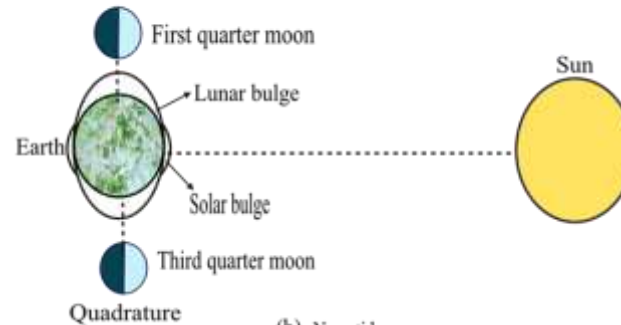# Spring-Neap Cycle of tides

Neap–spring tidal cycles, the result of the phase changes of the Moon, are the most pronounced of these.

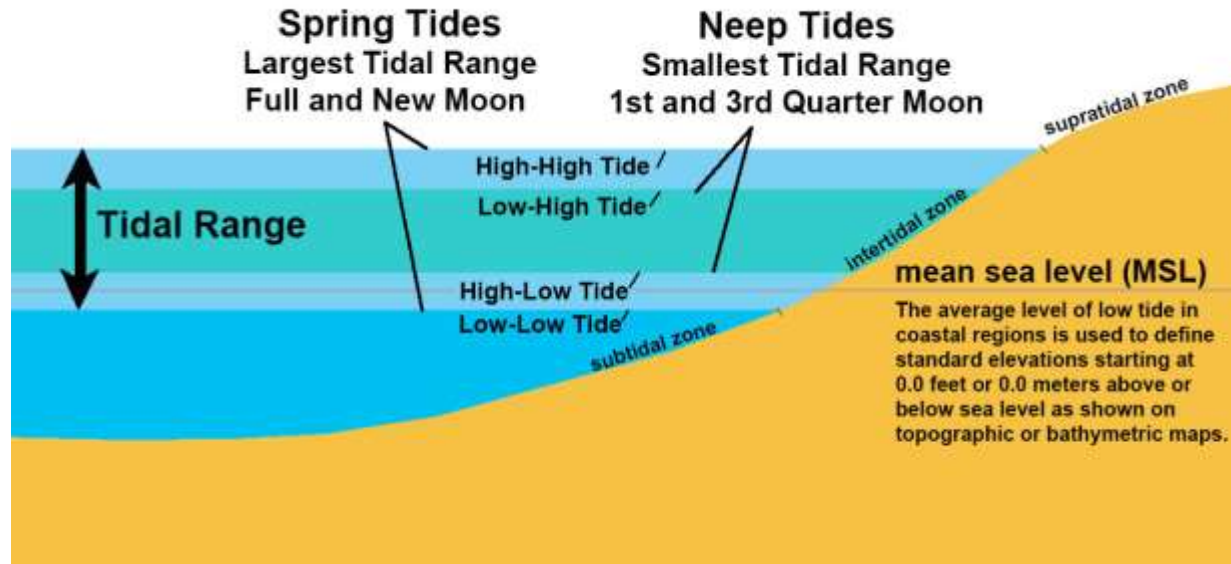**Spring tides occur every 14.76 days**

Day	1	8	15	22	29
Moon phase	Full	3rd quarter	New	1st quarter	Full
Tide phase	Spring	Neap	Spring	Neap	Spring

(a) Spring tides

(b) Neap tides

Tidal ranges during spring-neap cycle

Spring Tides
Largest Tidal Range
Full and New Moon

Neep Tides
Smallest Tidal Range
1st and 3rd Quarter Moon

supratidal zone

Tidal Range

High-High Tide
Low-High Tide

intertidal zone

mean sea level (MSL)

High-Low Tide
Low-Low Tide

subtidal zone

The average level of low tide in coastal regions is used to define standard elevations starting at 0.0 feet or 0.0 meters above or below sea level as shown on topographic or bathymetric maps.

Major tidal frequencies

Tidal variability can be represented as a sum of different constituents.

Each constituent represents a periodic change or variation in the relative positions of the Earth, Moon and Sun.

The frequencies are determined by the cycles in the motions of moon, sun and earth.

TABLE 1.1: Details of the major tidal constituents and their period.

Constituents	Name and Origin	Period
Semidiurnal		
M_2	Principal Lunar	12.421 hours
S2	Principal Solar	12.000 hours
N2	Elliptical Lunar	12.658 hours
K2	Declination Luni-Solar	11.967 hours
Dirnal		
K1	Declination Luni-Solar	23.93 hours
O1	Principal Lunar	25.82 hours
P1	Principal Solar	24.07 hours
Q1	Elliptical Lunar	26.87 hours
Long-Period		
Mf	Fortnightly Lunar	13.661 days
Mm	Monthly Lunar	27.555 days
Msa	Semiannual Solar	182.621 days

Harmonic Analysis

The mathematical process by which the observed tide or tidal current at any place is separated into basic harmonic constituents.

Tidal variations can be represented as a sum of finite number of harmonics

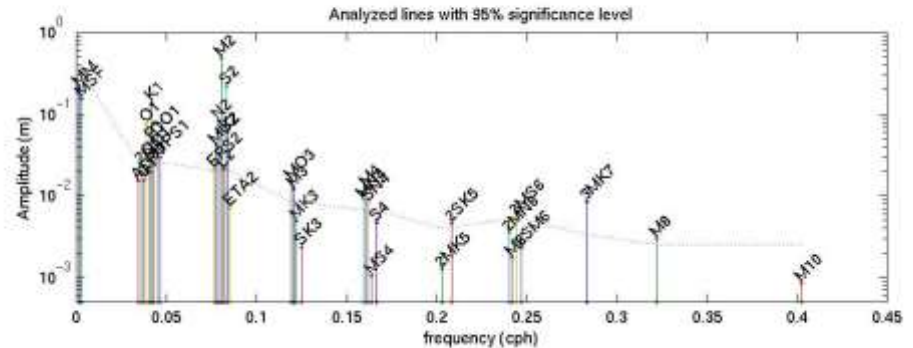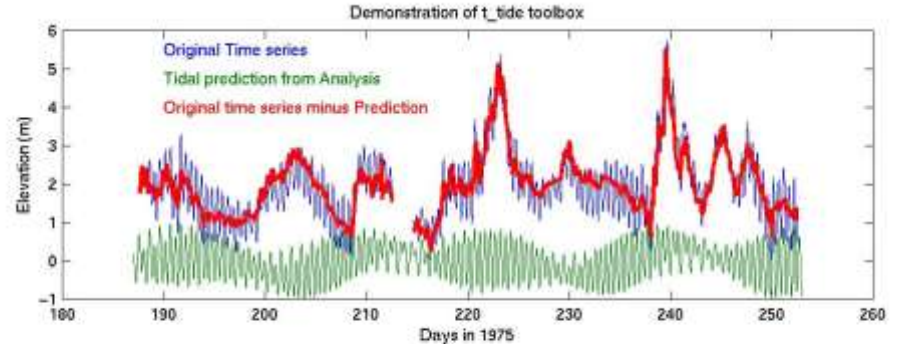Application of Fourier analysis to the tidal motions : harmonic analysis (William Thomson's)

TOOLS

TASK (PSMSL/POL Tidal Analysis Software Kit 2000**)**

T_TIDE (Pawlowicz's **et al., 2002)**

U_tide
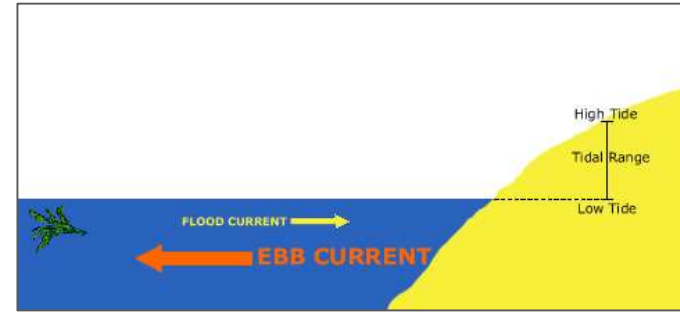
(fortran, matlab, Python)

Tidal currents and tidal ellipses

Tidal currents : Horizontal flow accompanied by rise and fall of tide

Tidal currents can be expressed in terms of ellipses.

Semimajor axis of the ellipse represents the maximum amplitude of tidal current.
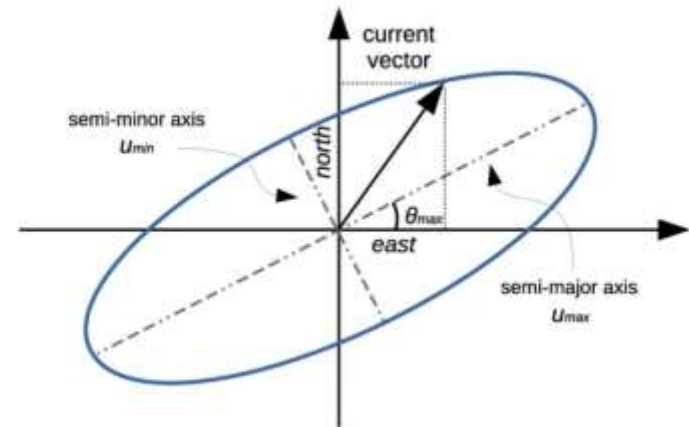
Numerical Modelling of barotropic tides

- **Sir Isaac Newton** was the first who developed the tide-generating force based on gravitational theory and provided an explanation for the cause of tides (**Equilibrium theory**).
- Later, **Pierre-Simon Laplace**, a French mathematician, introduced the dynamical theory of tides by considering the dynamical nature of tide generating force, rotational effects and gravity (**Dynamical theory**).
- He formulated the hydrodynamical equation for tides, known as **Laplace Tidal Equations (LTE)** in 1775 and explained many realistic features of tides in the ocean basins including amphidromic systems.
- However, **solving the LTE was difficult without simplifying the equations** and therefore **prediction of tides based on simplified LTE in the coastal regions was not accurate** for practical applications.

Numerical models

- A phenomenal progress in the study of tides was made with the emergence of numerical ocean modelling using digital computers in the second half of the 20th century.

- Many researchers attempted to **derive solutions of LTE numerically** and prepared the global maps of ocean tides.

- The **initial attempts on global tidal modelling were focused on mapping the semidiurnal tides** (M_2 and S_2) in the open ocean using coarse grid resolutions, while shallow coastal regions were ignored (Bogdanov and Magarik, 1967; Pekeris and Accad, 1969; Schwiderski, 1979).

Barotropic tidal modelling : Basic equations

Tides are shallow water waves. The model consists of a system of vertically integrated continuity equation and the equations of momentum.

$$\frac{\partial \eta}{\partial t} + \frac{\partial U}{\partial x} + \frac{\partial V}{\partial y} = 0 \tag{1}$$

Frictional term   Viscous term

$$\frac{\partial U}{\partial t} + \frac{\partial}{\partial x}(uU) - \frac{\partial}{\partial y}(vU) - fV = -gH\frac{\partial \eta}{\partial x} - \frac{C_d U \sqrt{U^2 + V^2}}{H^2} + A_H \left(\frac{\partial^2 U}{\partial x^2} + \frac{\partial^2 U}{\partial y^2} \right) \tag{2}$$

$$\frac{\partial V}{\partial t} + \frac{\partial}{\partial x}(uV) + \frac{\partial}{\partial y}(vV) + fU = -gH\frac{\partial \eta}{\partial y} - \frac{C_d V \sqrt{U^2 + V^2}}{H^2} + A_H \left(\frac{\partial^2 V}{\partial x^2} + \frac{\partial^2 V}{\partial y^2} \right) \tag{3}$$

The numerical solution of the equations is obtained by discretizing the equations in space using an explicit finite difference scheme over a numerical grid and in time.

The model requires detailed bathymetry (water depth data) for the model domain, a definition of the initial sea state usually just a still water level, and some data to force the model.

For a tidal model the forcing data will usually be the known tides around the edge of the model – a surge model would also include wind data and atmospheric pressure data.

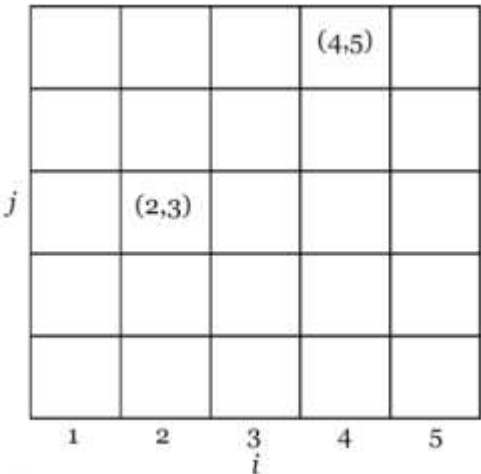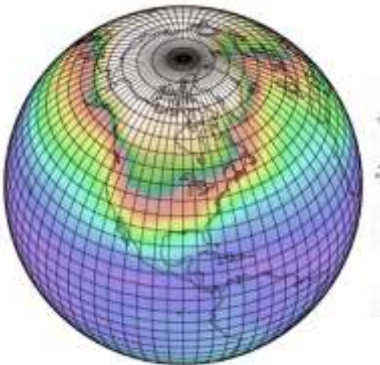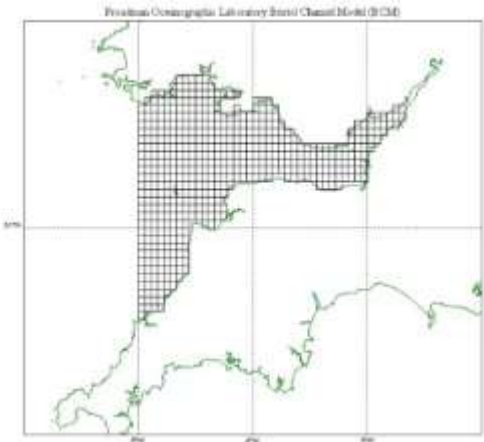The model will then use the equations governing fluid flow to compute the tidal level and currents for the required period of time


Figure 3: a two-dimensional model grid

- **Parke and Hender-shott (1980)** were the first who derived more realistic maps of M2 and K1 tides in the global ocean.
- In order to obtain more accurate global tidal solutions, Schwiderski (1980a) adopted a novel approach, i.e. **the assimilation of Island and coastal tide gauge data into a hydrodynamic model**, which was a major milestone in the global tidal modelling.
- Schwiderski (1980a, 1983) **assimilated about 2000 coastal tide gauge data into a global hydrodynamic model with a grid resolution of 1◦ x1◦** and prepared global tidal charts for 10 major tidal constituents (diurnal, semidiurnal and long period tides), which was one of the first reliable global tidal solutions.
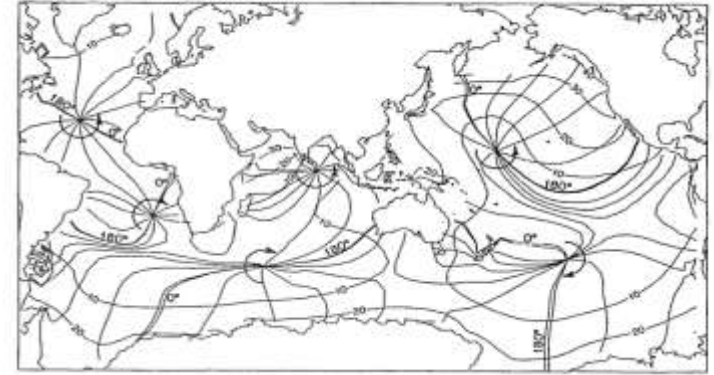
Parke and Hender-shott (1980)
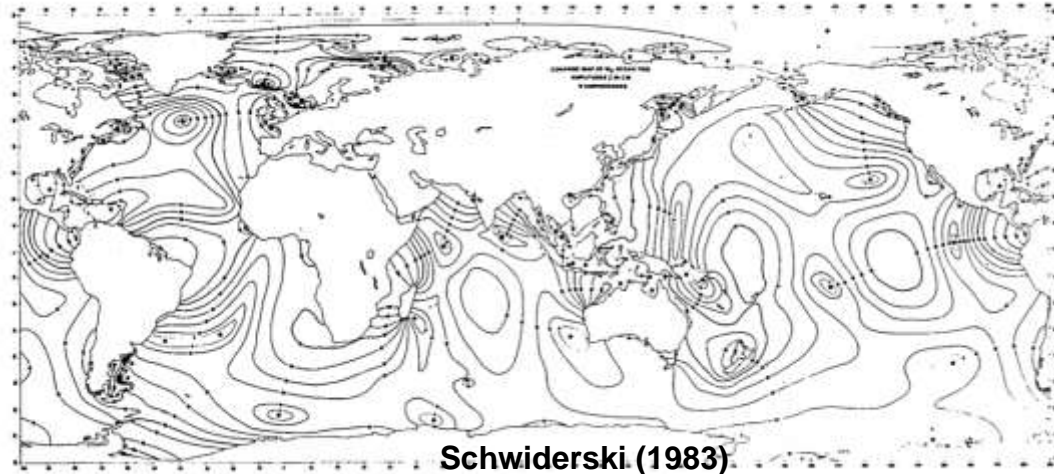
Schwiderski (1983)

The inaccuracies in the bathymetry and poor representation of coastal and shallow regions in the model restricted its use in the coastal and geophysical applications.
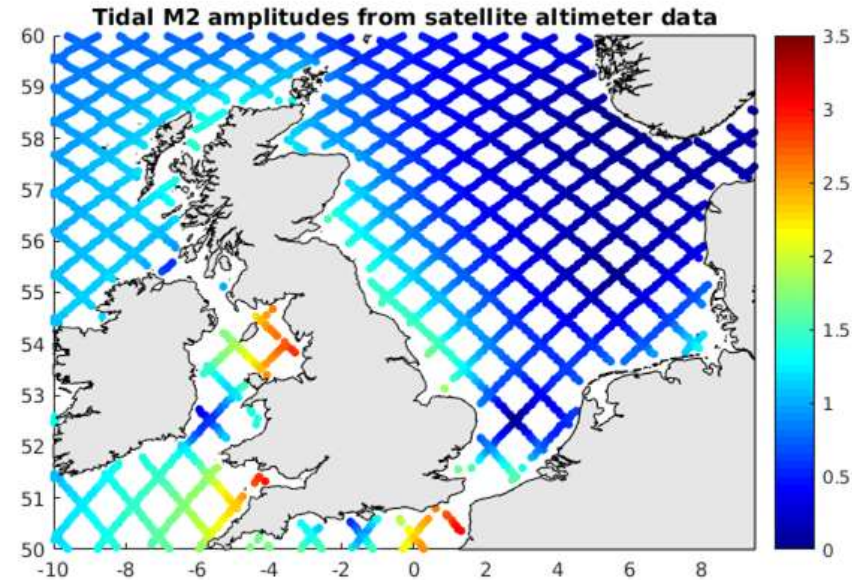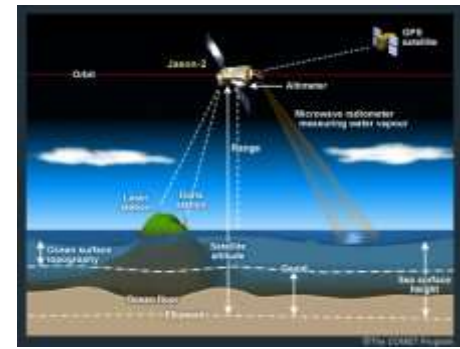
Tides from satellite altimetry

A better understanding of global distribution of tides and **unprecedented increase in the accuracy of the global tidal maps is achieved by the measurements of sea surface height using satellite altimetry.**

Cartwright and Ray (1990, 1991) extracted the tidal signals from altimeter observations obtained from the **Geosat satellite**, which was launched in 1985.

Even though the tidal solutions from Geosat were better than numerical models at that time, **it had limitations due to short data record and orbital errors.**

Later, more accurate global tidal maps were made available with the launch of the **high precision altimeter mission, Topex/Poseidon (T/P)**, in 1992 and followed **by Jason-1 and 2** (Schrama and Ray, 1994).

Many researchers used this data in the subsequent years and prepared more accurate global empirical tidal solutions based on altimeter (Ma et al., 1994; Desai and Wahr, 1995).

Tidal M2 amplitudes from satellite altimeter data

How tidal signals are extracted from satellite altimeter : Tidal frequency aliasing

- **Tides have diurnal and semidiurnal periods but satellite repeat cycle is couple of days. For Topex/Poseidon satellites period is 10 days.**

- **So, tidal signals from satellite altimeter is extracted by aliasing tidal periods into higher periods, called tidal frequency aliasing.**

- **For the TOPEX/Poseidon mission, aliasing period is 62.11 and 58.74 days for the M_2 and S_2 tidal constituents respectively.**

$$\frac{1}{T_a} = abs\left[mod\left(\frac{1}{T_k} + \frac{1}{T_N}, \frac{2}{N}\right) - \frac{1}{T_N}\right]$$

$2T_N$ = Sampling interval (Nyquist frequency)

T_k = Period of tidal signal

Adequately Sampled Signal

Aliased Signal Due to Undersampling

(Parke et al., 1987).
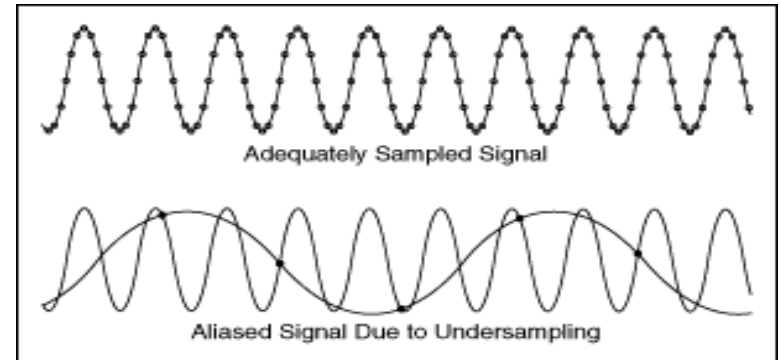
Egbert et al. (1994) prepared the global tidal solutions **(TPXO)** using assimilation of satellite data into hydrodynamic models and it was updated in the following years with the availability of **more accurate tidal solutions from altimeter data** (Egbert and Erofeeva (2002a), TPXO7/8/9 : https : //www.tpxo.net/home).

- **More accurate estimation of barotropic energy fluxes**

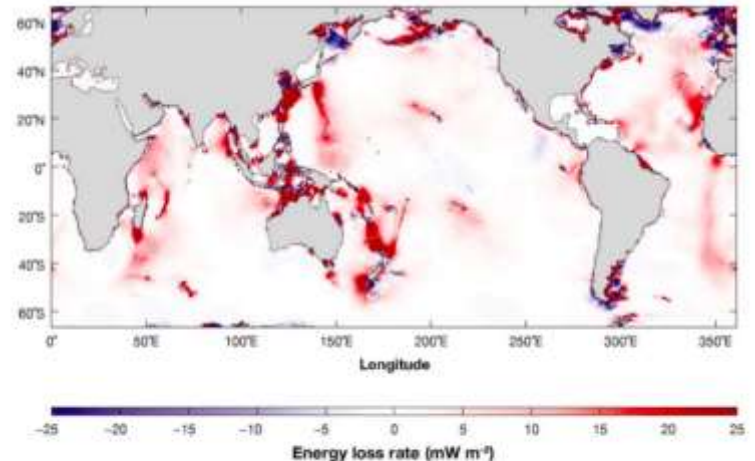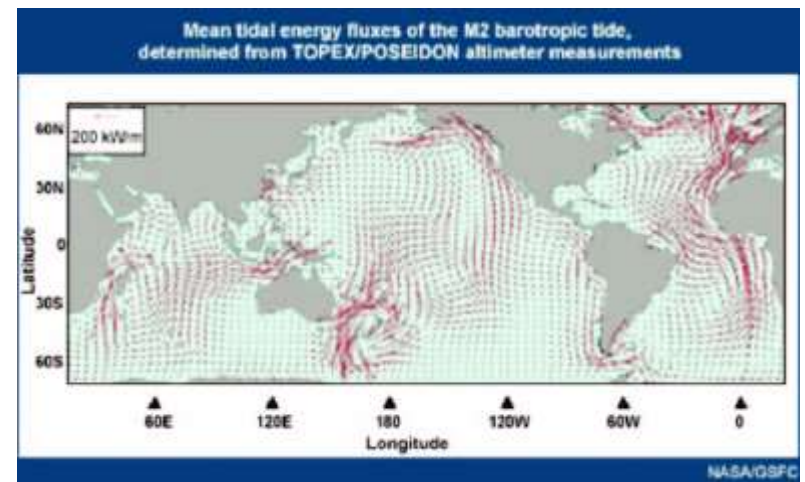- **Identification of significant loss of tidal energy in the deep ocean 33% via internal tide generation**

FIGURE 1.2: Barotropic tidal energy dissipation of M_2 tides in the global ocean (Source : Egbert and Ray (2000a)).

TPXO Global tidal Models

TPXO is a series of fully-global models of ocean tides, **which best-fits, in a least-squares sense, the Laplace Tidal Equations and altimetry data.** Each next model in TPXO series is based on updated bathymetry and assimilates more data compared to previous versions.

The TPXO models include complex amplitudes of MSL-relative sea-surface elevations and transports/currents for eight primary (M2, S2, N2, K2, K1, O1, P1, Q1), two long period (Mf,Mm) and 3 non-linear (M4, MS4, MN4) harmonic constituents (plus 2N2 and S1 for TPXO9 only).

Available at
https://www.tpxo.net/global
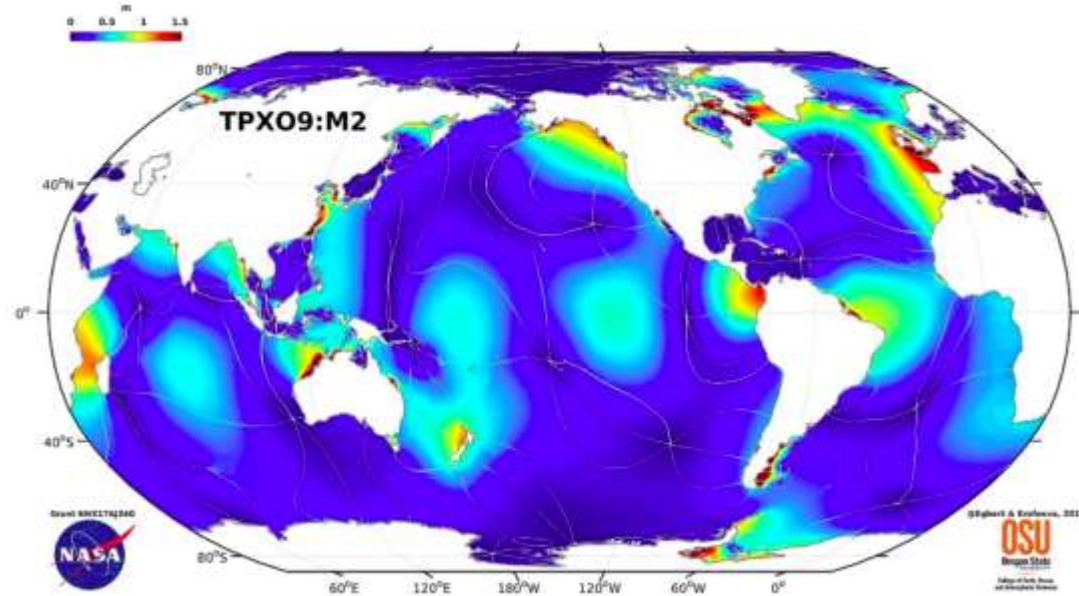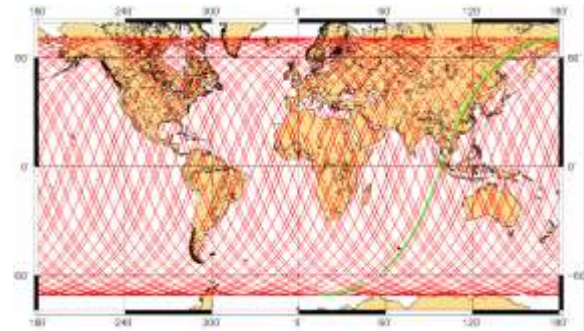
Other global tidal models

OTPS

Since then, many global tidal models, **such as GOT99.2 (Ray, 1999), FES2004 (Lyard et al., 2006) and FES2012 (Carrère et al., 2012),** were developed in the following years by data assimilation, higher horizontal resolution and inclusion of more tidal constituents.

A detailed review on the development and accuracy of the global tidal models is available in Stammer et al. (2014).
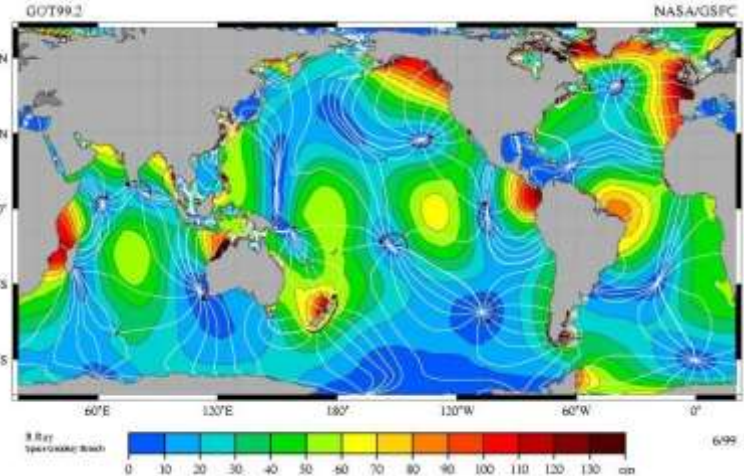
FES2004
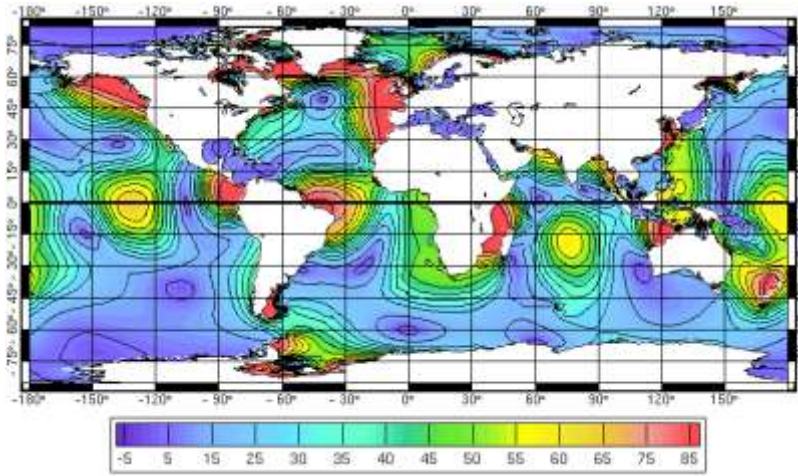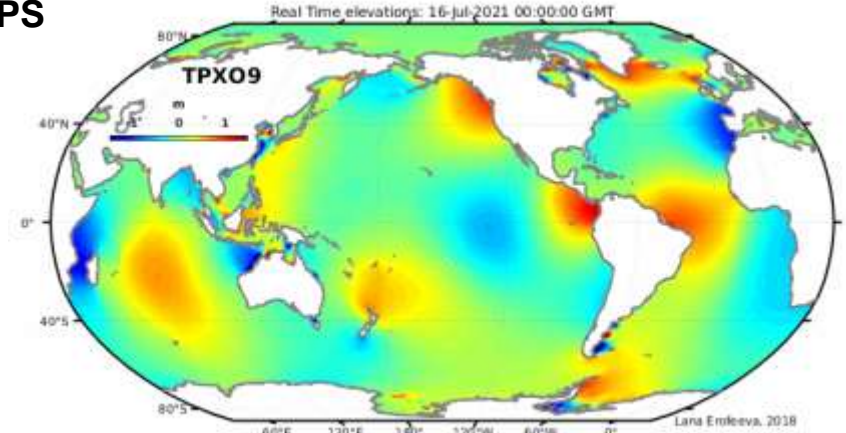
GOT99.2

Parallel to the development of satellite-based global tidal solutions, **pure hydrodynamical models with finite element mesh, with higher grid resolution in the coastal and shallow seas, were also being developed.**

One of the pioneering works on this was done by **Le Provost et al. (1994), in which they used a finite element hydrodynamic model with assimilation of altimeter data, and derived more accurate global tidal maps.**

The next important development of the global tidal modelling was combined use of satellite altimetry data, coastal tide gauges and hydrodynamical models by using the data assimilation techniques (Egbert et al., 1994; Kantha, 1995; Shum et al., 1997).
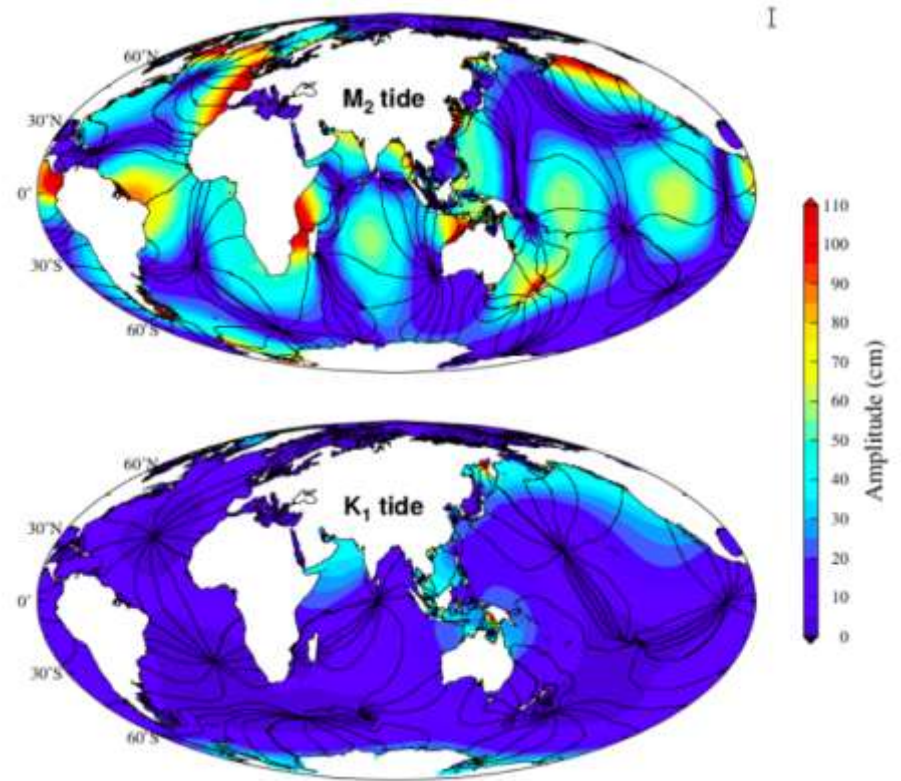
Initial conditions
 Usually starts from zero

Tides as Boundary conditions

Elevations

Time series and spectral values (amplitude and phase of tidal constituents) from global models at open boundaries

ROMS : both elevation and currents as amplitude and phase of elevation and currents in complex form
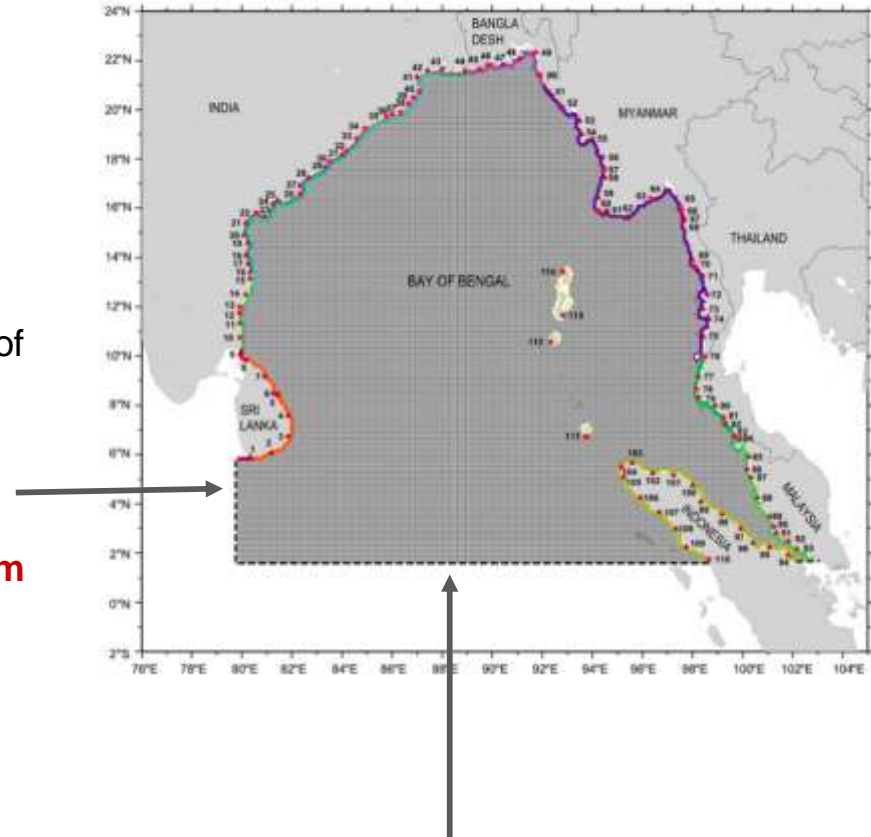
ADCIRC and FVCOM : tidal elevation

Tidal currents
 **For regional applications**
Tides as body force (MOM)
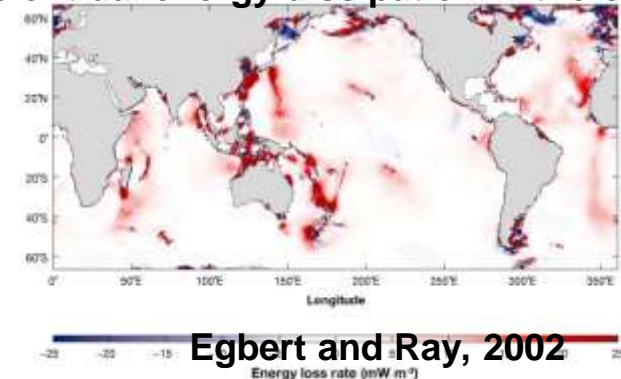   Tidal potential
 For global models

Barotropic and internal tides in the Ocean

Barotropic tides

- Periodic rise and fall of ocean surface caused by the gravitational force exerted by the sun and moon and the rotation of earth-moon-sun system.

- Tidal oscillations are combinations of waves having different frequencies, known as tidal harmonics.

- Origin of Constituents : Linked to the relative position or rotation of the Sun Earth.

   - The dominant periodicities

        Half a day (semidiurnal)

        One day (diurnal).

   - Main constituents

        Semidiurnal   : M_2, S_2 and N_2

        Diurnal   : K_1 and O_1.

   - Tidal currents :   Horizontal tidal flow
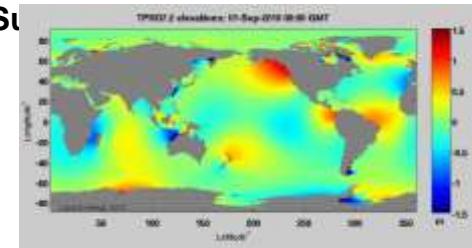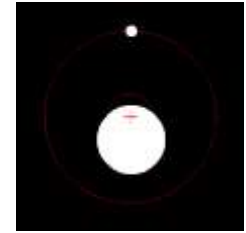
What happens to the tidal energy in the ocean ? what are the implications ?

- Tides lose about 3.5 TW energy in the ocean.

- Dissipates by means of bottom drag in the shallow seas (2.5TW).

- Conversion into Baroclinic over topography
   internal tide generation (about 1 TW)

Map of tidal energy dissipation in the ocean


Egbert and Ray, 2002

Energy loss rate (mW m⁻²)

How tides generate internal waves ?

- Internal tides are **internal gravity waves at tidal periods generated due to interaction of barotropic tides with steep topographic** features such as continental slopes and submarine ridges.

- Once they are generated over the topography, they can freely propagate into larger distances across the ocean.

- The presence of these internal waves can be detected from temperature and velocity
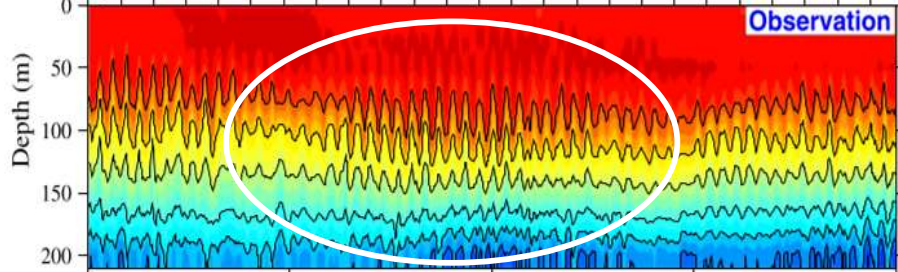
Importance

- **Ocean Mixing**
  Half of the energy for interior mixing.
  Maintain the stratification
- **Nutrient distribution**
- **Biological Productivity and ecosystem**
- **Sediment transport**
- **Sound Propagation**
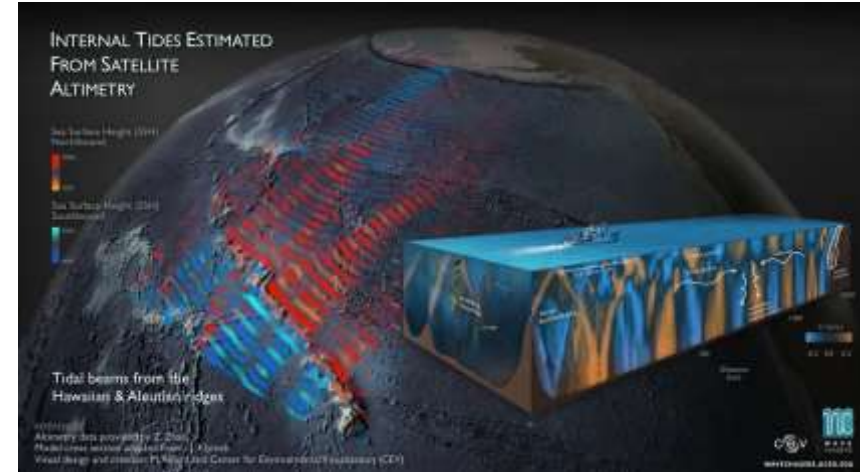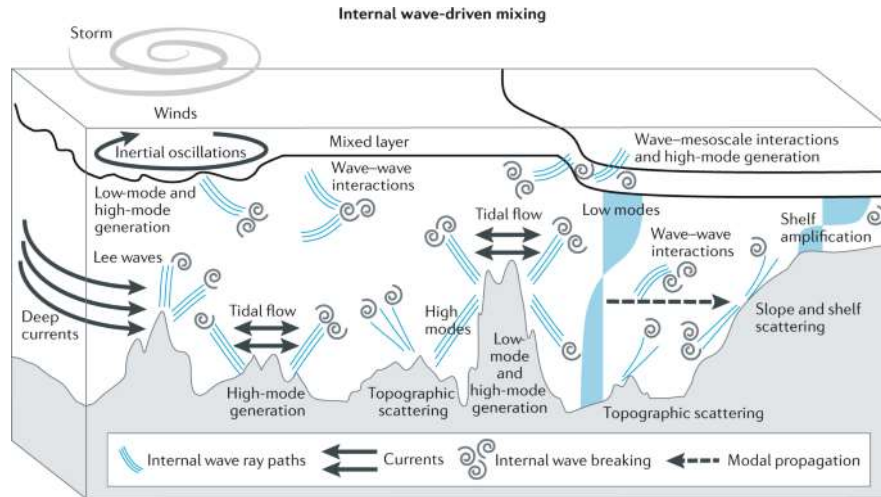- **Offshore industries**
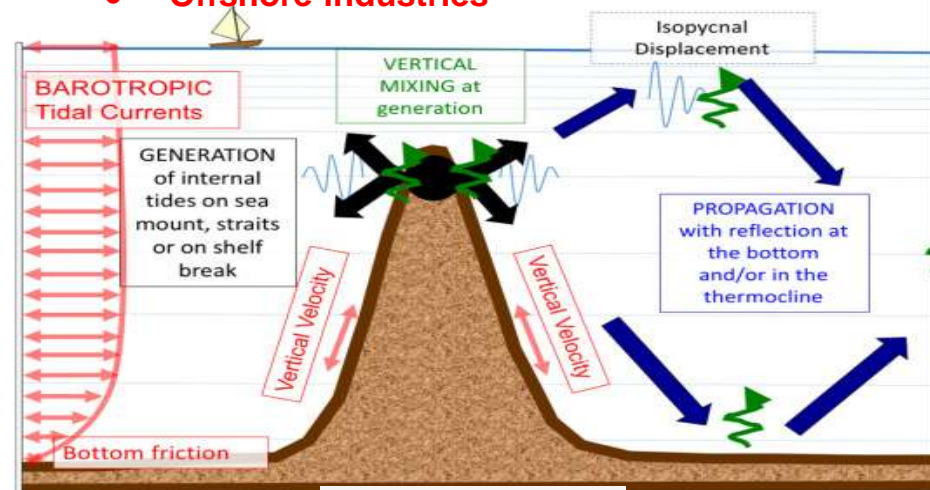
Nugroho et al., 2018

Propagation of internal tides in the ocean

Propagate 1000's of km
Without much dissipation

About 30 % of the energy dissipates near the
generation sites

Internal wave-driven mixing

INTERNAL TIDES ESTIMATED FROM SATELLITE ALTIMETRY

Tidal beams from the Hawaiian & Aleutian ridges

Propagation of internal tides on the continental slope

$$Criticality = \frac{Topographic\ slope\ (\gamma)}{Slope\ of\ internal\ wave\ characteristics\ (c)}$$

where the slope of internal wave characteristics is given by,

$$c = \left(\frac{\omega^2 - f^2}{N^2 - \omega^2}\right)^{1/2}$$
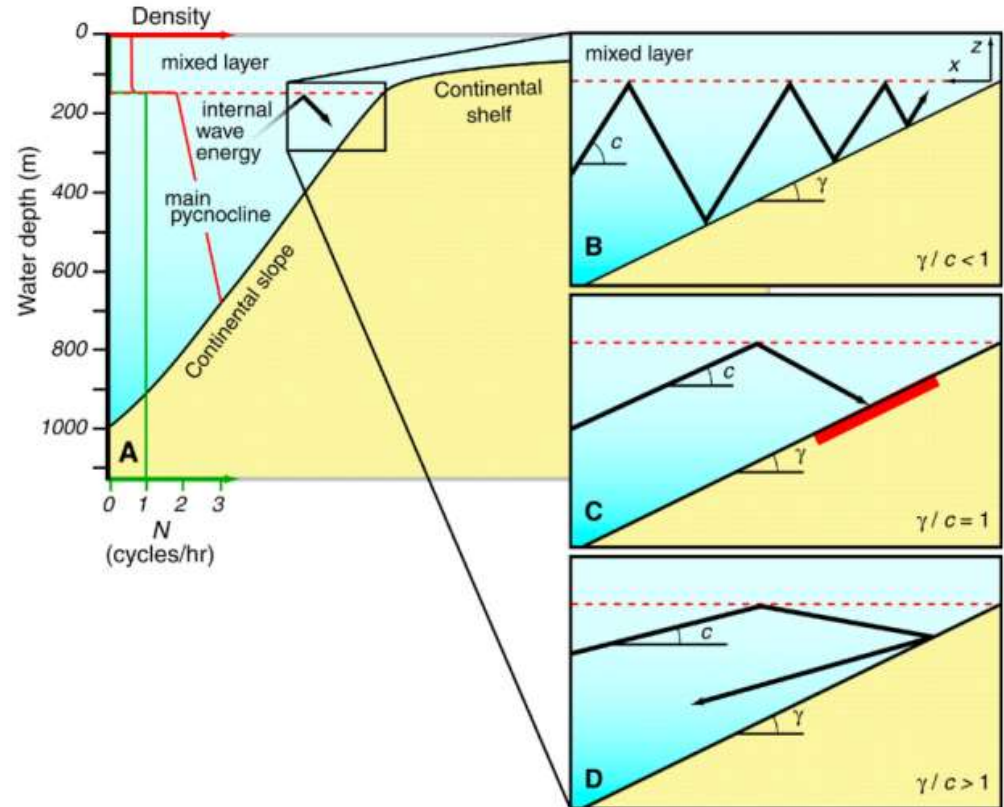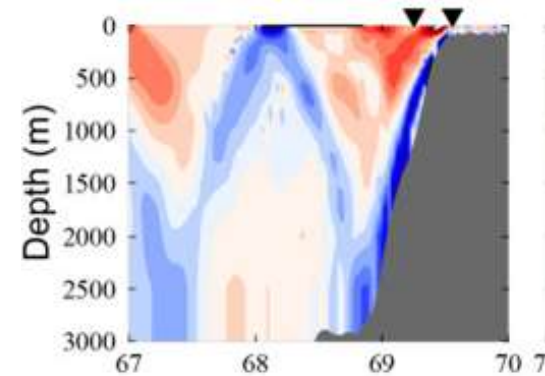
Modelling of internal tides

- **Initial attempts to simulate internal tides numerically across the oceanic ridges and continental margins were conducted using two-dimensional (2D) finite difference models (1980's)**
- **For example, numerical 2D models were used to simulate the internal tide generation in the Maline Shelf (Sherwin and Taylor, 1990) and the Bay of Biscay (Serpette and Mazé, 1989). These studies identified onshore and offshore propagation of internal tides from the shelf break and beam-like propagation of internal tide due to scattering of internal tides into higher vertical modes in the continental margins.**
- **In addition, these studies also suggested the possibility of strong internal tide mixing near the generation sites, which is later confirmed by in-situ observations.**

- **Using POM (Princeton Ocean Model) configured for the Australian North West Shelf, Holloway (1996) suggested that three-dimensional (3D) effects are important for the accurate prediction of internal tide amplitude.**
- **Later, many researchers implemented 3D models to study the internal tide generation at many regions around the world oceans (Cummins and Oey, 1997; Niwa and Hibiya, 2001; Holloway et al., 2001; Merrifield and Holloway, 2002)**

The **first global internal tide fields from numerical models were computed by Arbic et al. (2004) and Simmons et al. (2004b)**. Though solutions were based on a two-layer model with a coarse horizontal resolution (1/4 ◦), the energy conversion and tidal dissipation in the model were close to the observed values obtained from satellite altimeters.

Arbic et al. (2004)

Simmons (2008) studied M2 internal tide generation in the global ocean with realistic bathymetry, higher horizontal grid resolution (1/8 ◦) and vertical levels (16 levels). They noticed energy transfer from M_2 internal tides into its higher and sub harmonics and enhanced mixing in the turning latitudes due to Parametric Subharmonic Instability (PSI).
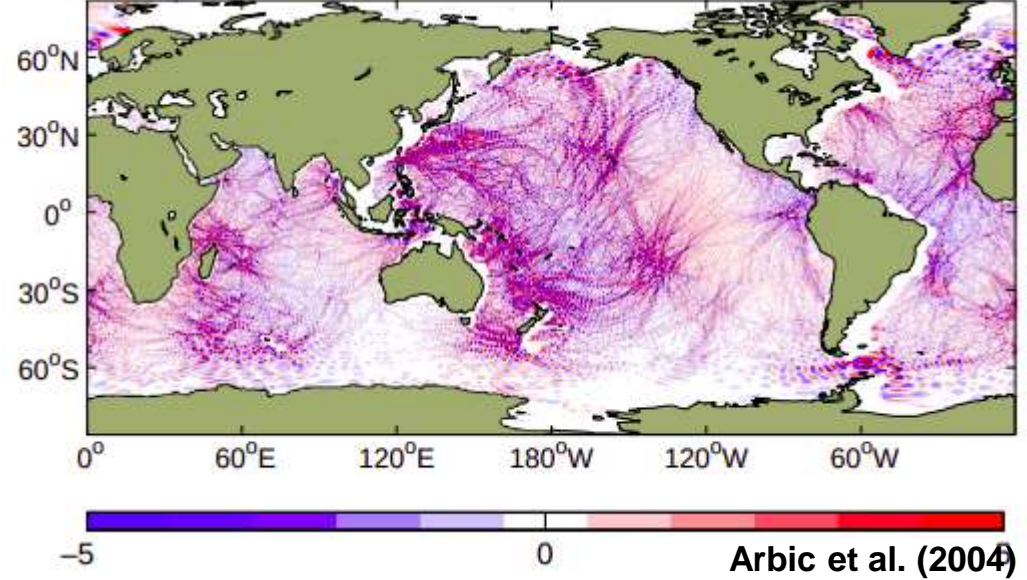
In these early global internal tide models, stratification was considered to be horizontally uniform and atmospheric forcing was absent.

Arbic et al. (2010, 2012) used an eddy-resolving model with a resolution of 1/12.5 ◦ and 32 vertical levels by realistic atmospheric forcing to simulate the internal tides in the global ocean. They noted that realistic horizontal variation of the stratification in the model considerably improved the internal tide field.
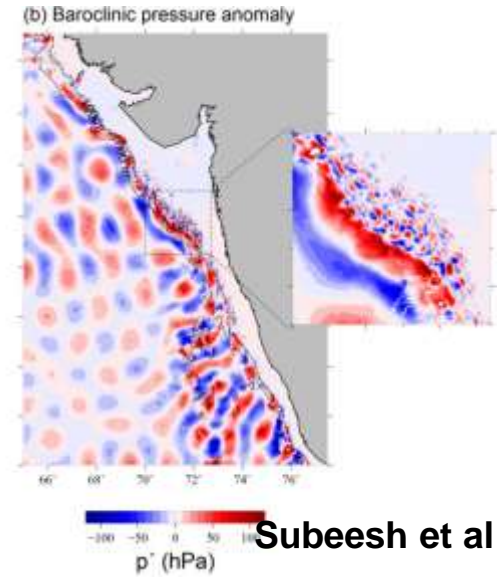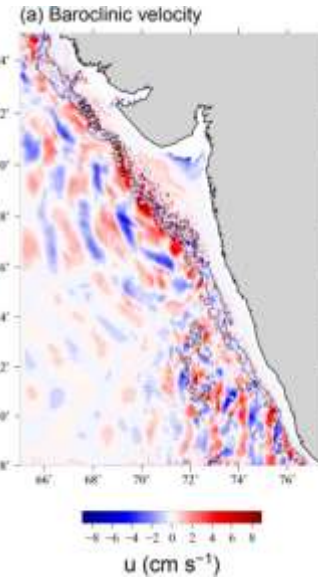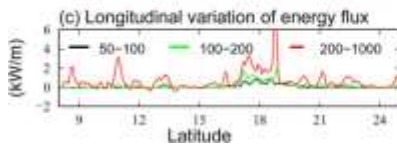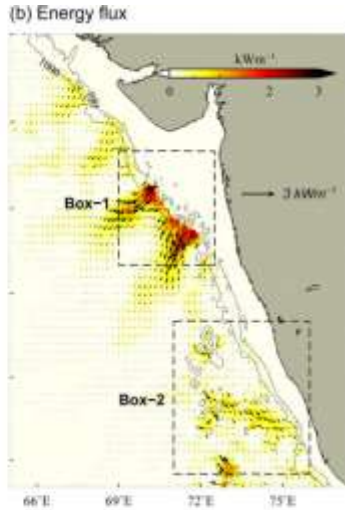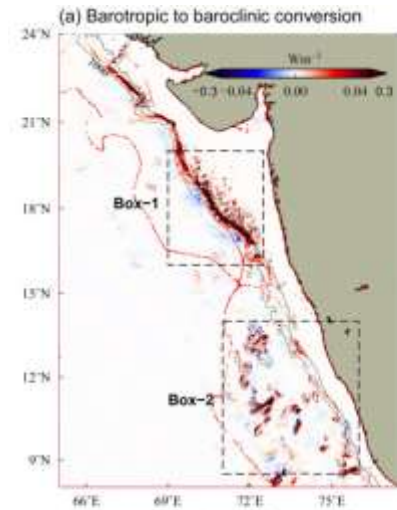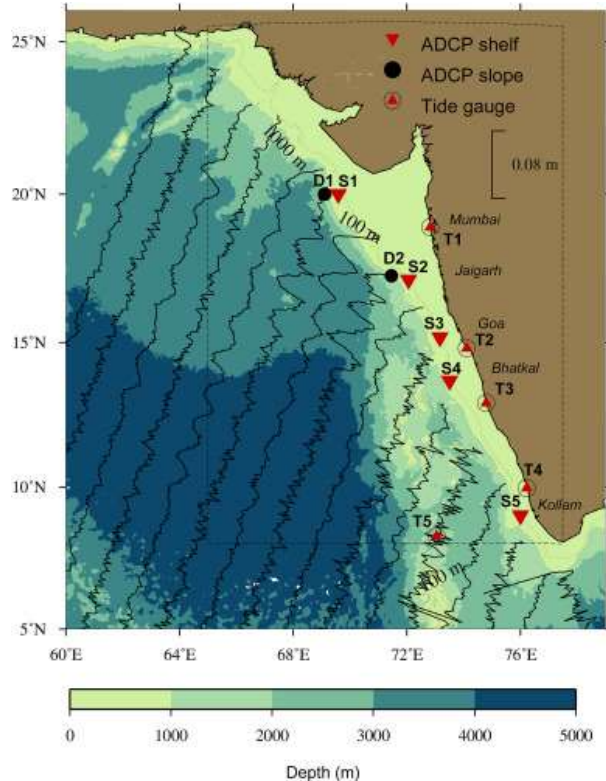
Subeesh et al (2020)

**The total barotropic to baroclinic conversion of M₂ tidal constituent is about 2.4 GW.**

The regions of shelf breaks and upper slope around 16–18.5° N and the northern part of the Chagos-Laccadive Ridge (8–14° N) are the two most important regions of internal tide generation along the WCI, which together contribute to more than 50% of total area-integrated M₂

Modelling of barotropic and internal tides along the Indian Coasts

West coast of India

**Observed and modelled barotropic tidal currents**
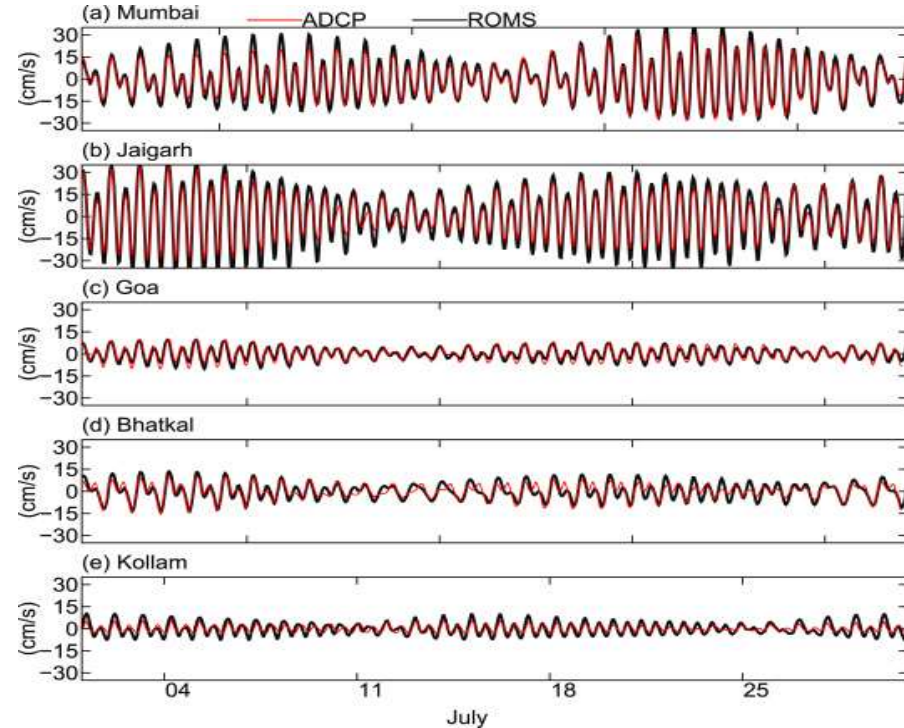
Subeesh et al (2020)

Observed barotropic and internal tides on the continental shelf in the western Bay of Bengal

- **ADCP Observations show that currents in the tidal band contribute about 5-14% of the total currents on the shelf.**

- **Dominant part of the tidal variability is contributed by baroclinic tidal currents on the shelf-break**

ADCP Location	Barotropic (%)	Baroclinic (%)	Total (%)
CD	3.6	10.3	14
RM	2.6	5.4	8
KN	1.6	4.0	5.6
SVP	2.8	1.7	4.5
VP	2.5	2.7	5.2
SGP	2.4	6.2	8.6
GP	3.5	10.4	13.9
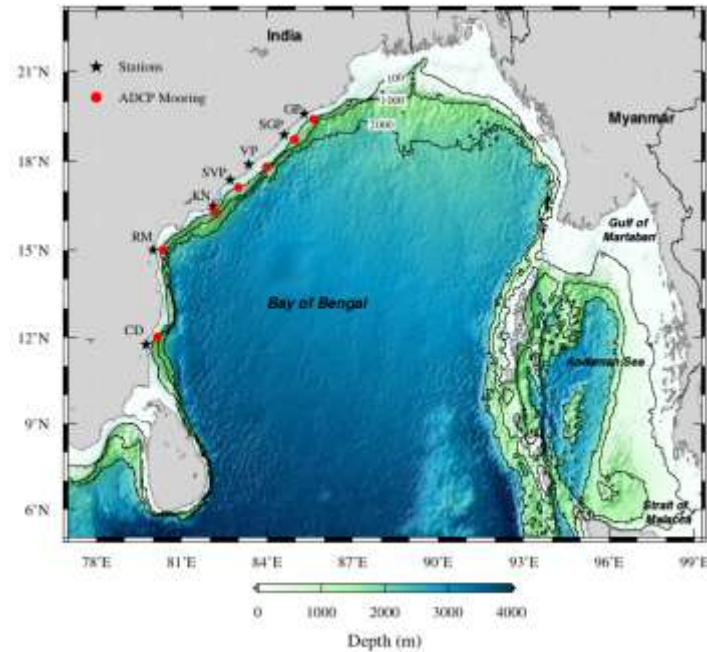
% of contribution of barotropic and baroclinic tidal currents
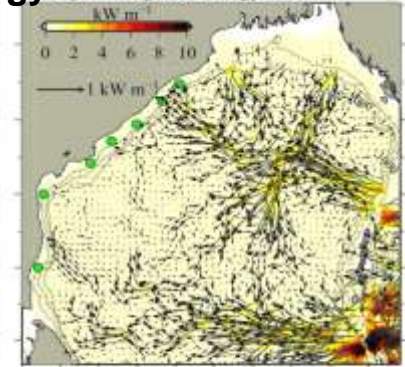
1) Generation and propagation of internal tides in the Bay of Bengal

- Conversion rates along the western BoB are very small.

- Major Sources : **Continental slopes in the head of the bay and AN Ridge**

- Two beams from AN Ridge

- Internal tides propagate with a speed of about 2.5 cm/s and they take about 5-6 days to reach the shelf in the northwestern BoB.
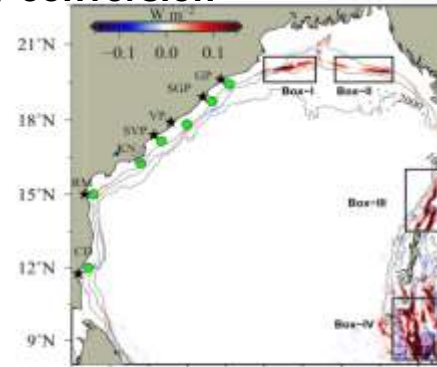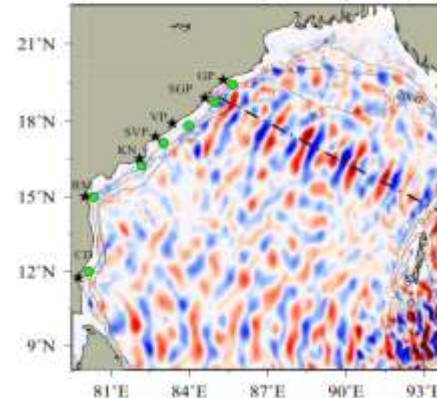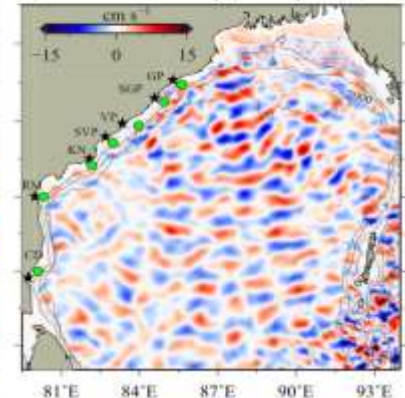
Energy conversion   **Energy flux**
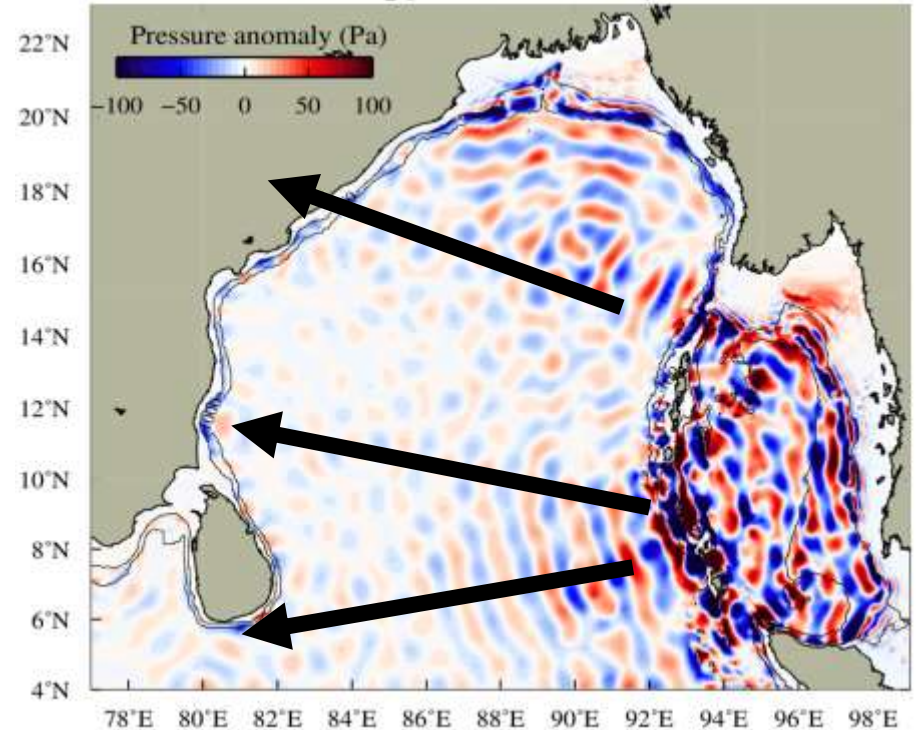

c) Baroclinic velocity (u component)   d) Baroclinic velocity (v component)

1) Generation and propagation of internal tides in the Bay of Bengal

Animation of internal tide generation and propagation in the BoB

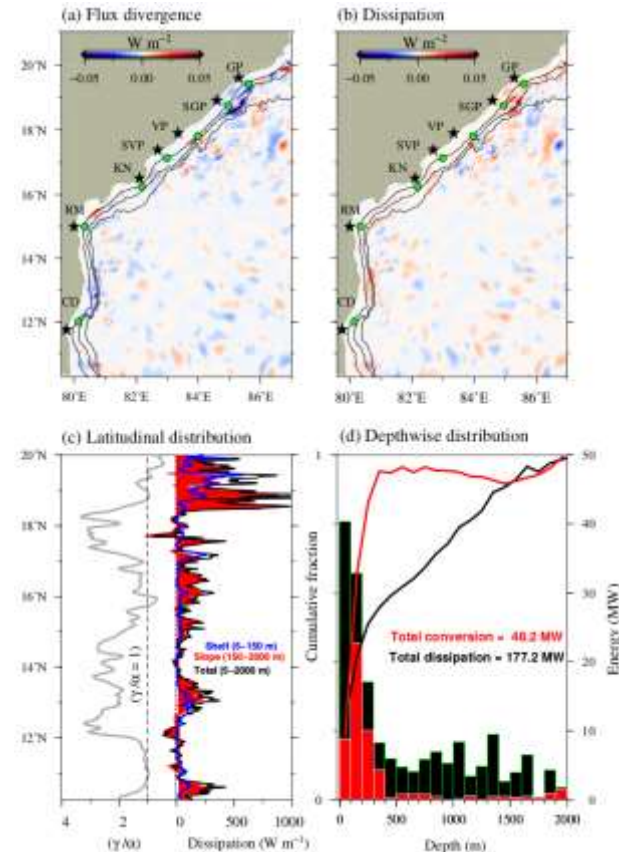**2) How the onshore transmission of internal tides varies along the western BoB**

- There are differences in the internal tide activity along the shelf.

- **Topographic slope in the western BoB determines the strength of internal tide activity along the shelf**
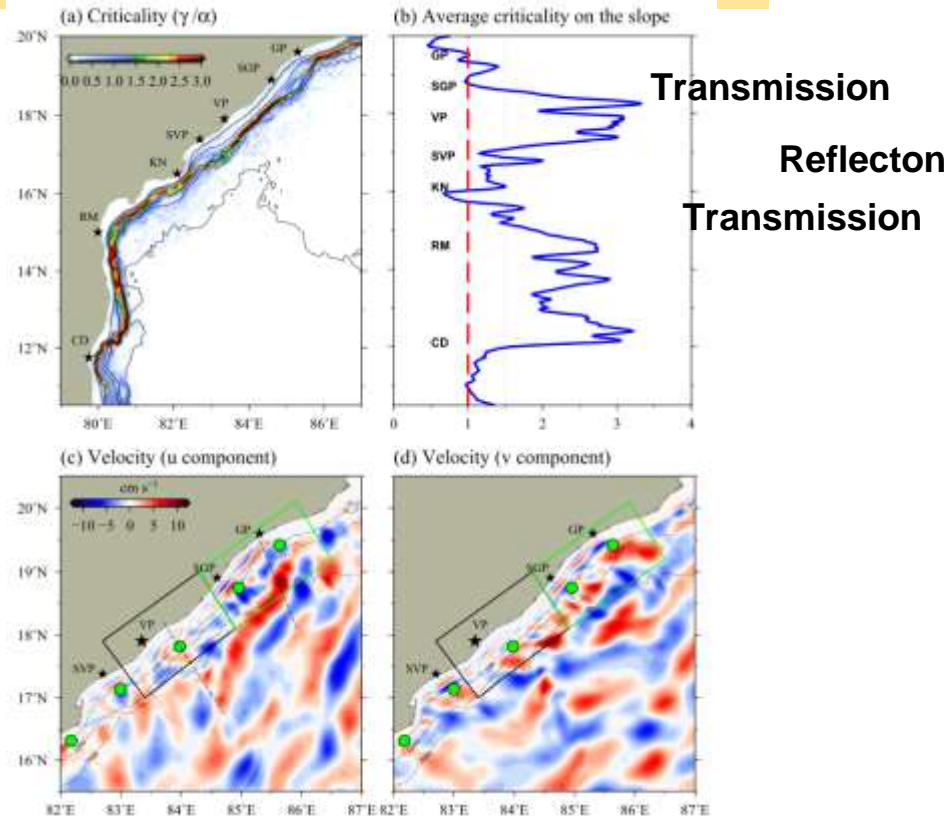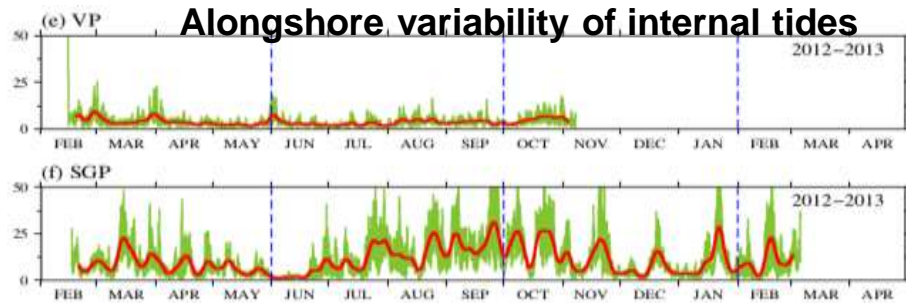
Alongshore variability of internal tides

Transmission

Reflecton

Transmission

4) Dissipation of internal tides along the western BoB

- **Energy dissipation on the slope is about two times larger than that on the shelf**

- **Total area integrated M2 dissipation in the western BoB (10.25⁰ - 20⁰N, 79⁰ - 87⁰E) which is 3 to 4 times larger than the local conversion (48.2 MW).**

- **This indicates that continental margins in the western BoB are sinks for remotely-generated internal tide energy rather than sources.**

- **Main results : Internal tides observed along the**

(a) Flux divergence

(b) Dissipation

(c) Latitudinal distribution

(d) Depthwise distribution

Total conversion = 48.2 MW
Total dissipation = 177.2 MW

Convergence of internal tides in the northern Bay of Bengal

1) Strong internal tide energy in the deeper parts of the BoB

- **Further I looked into the spatial variability of internal tides using model simulation.**

- **Model estimates of internal tide energy shows that there is strong internal tide activity in the central part of the northern BoB, which about 457 km away from the generation sites.**

- **To examine this spatial variability, internal tide signals from the satellite altimetry is used.**

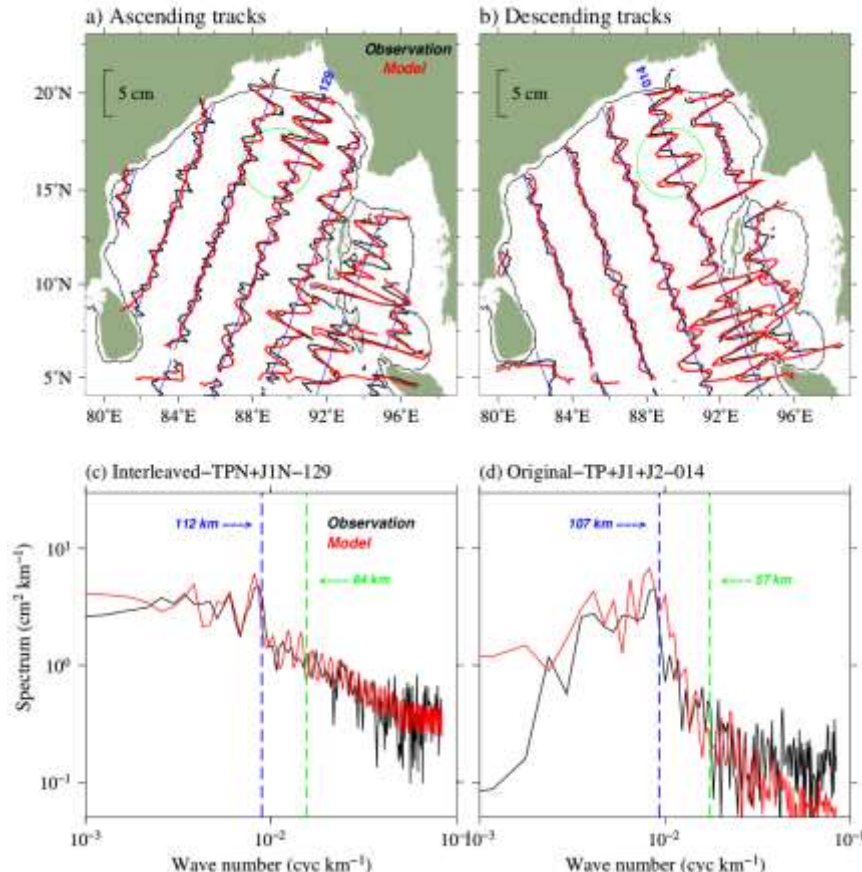M2 internal tide energy in the northern BoB
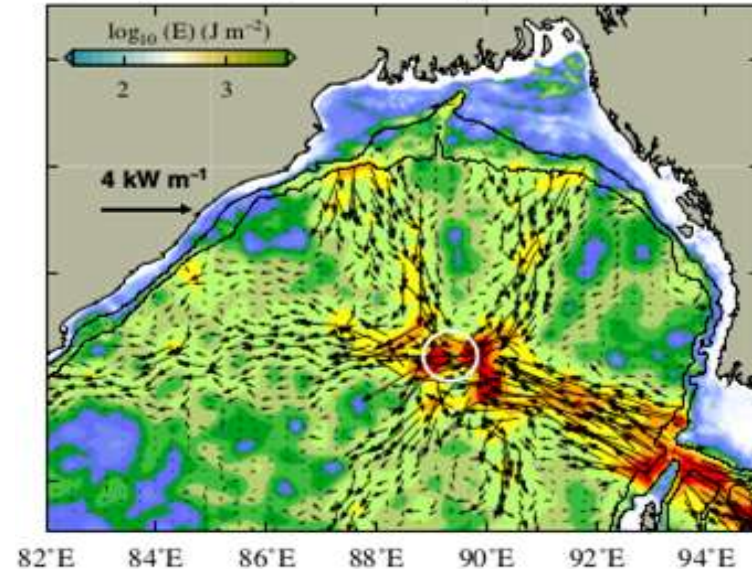
Convergence of internal tides in the northern Bay of Bengal

2) Surface amplitude of internal tides from satellite altimeter

● Relatively large SSH signals (2.5 to 3.5 cm) near the AN Ridge and adjacent to the continental slopes in the northern BoB.

● Presence of large amplitudes (2-3 cm) of M_2 internal tides in the deep regions of the north-central BoB.
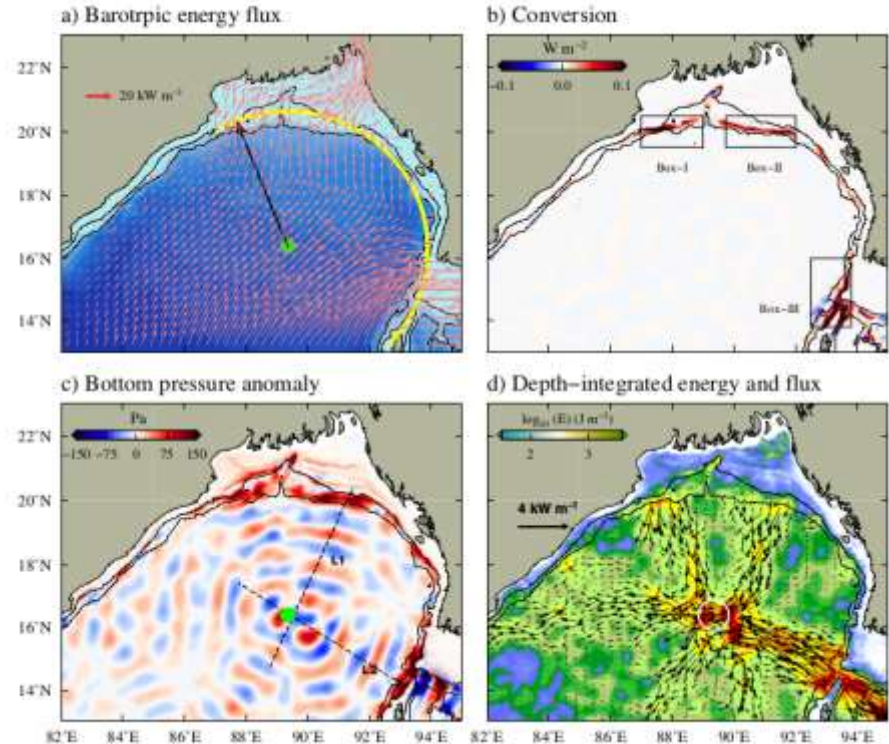
●nModel is able to simulate the spatial variability of M_2 internal tides in the BoB very well.

a) Ascending tracks   b) Descending tracks

(c) Interleaved−TPN+J1N−129   (d) Original−TP+J1+J2−014

3) Intensification of internal tides due to convergence of internal tides

- **Shape of the continental slopes in this region can be nearly described by a semi-circle.**

- **Internal tides radiating from the sources oriented in circular shape is converging into their focal region.**

- **This convergence results in the intensification of internal tides in the north-central BoB.**

- **We found enhanced energy dissipation in the focal region and such convergence can be cause strong dissipation in the ocean**

a) Barotrpic energy flux
b) Conversion
c) Bottom pressure anomaly
d) Depth-integrated energy and flux

1) Barotropic tides and its energy propagation in the Bay of Bengal and Andaman Sea

- Strong M_2 tidal currents with magnitudes of 50–100 cm s^{-1} are found over the wide continental shelves in the eastern AS and in the northern BoB.

- Strong tidal currents (50-70 cm s^{-1}) are also found across the AN Ridge.

- Magnitude of M_2 tidal currents is relatively small (less than 10 cm s^{-1}) along the continental margins of the western BoB, which is consistent with field

Barotropic M2 ellipse
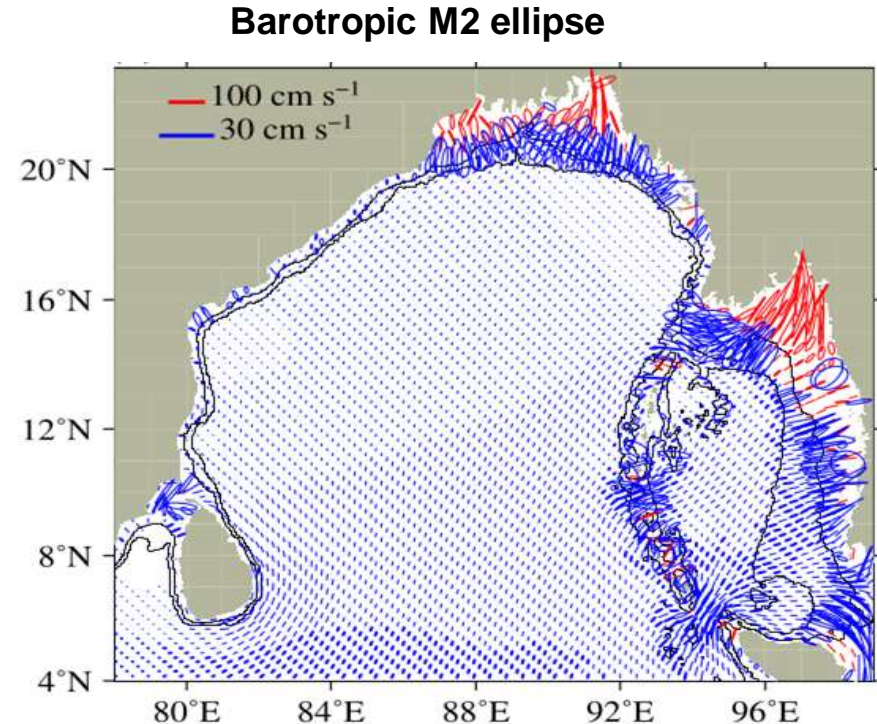
2) Barotropic tides and its energy dissipation in the Bay of Bengal and Andaman Sea

Simplified form of local tidal energy balance over a tidal period can be expressed as

$$W - \nabla \cdot F_b = Dissipation$$

W is the rate of work done by the gravitational force on the ocean and $\nabla \cdot Fb$ is the divergence of the barotropic energy flux F_b. Work done (*W*) by the tidal gravitational force can be neglected in the shallow marginal seas. Therefore, dissipation becomes balanced by divergence of barotropic energy flux.

Tidal energy Dissipation = Frictional dissipation + Internal tide generation

Internal tide Energy balance

$$\nabla \cdot \mathbf{F} + D = C$$

Frictional dissipation

$$\epsilon = \frac{k\rho}{T} \int_0^T [U_{bt}(t)^2 + V_{bt}(t)^2]^{3/2}$$

Internal energy flux

$$\mathbf{F} = \int_{-H}^{0} <\mathbf{u}'(z)\, p'(z)> dz$$

Rate of Energy conversion into internal tides

$$C = <\nabla H \cdot \mathbf{U}_{bt}\, p_b'>$$

3) Summary of M2 tidal energy budget in the Bay of Bengal and Andaman Sea

a) Conversion in BoB and AS

- Conversion at eight potential sources

    92.7% (17.71 GW)

- AN Ridge constitutes to about

    83.8% energy

- 94% of energy loss occurs by

    internal tides across AN Ridge
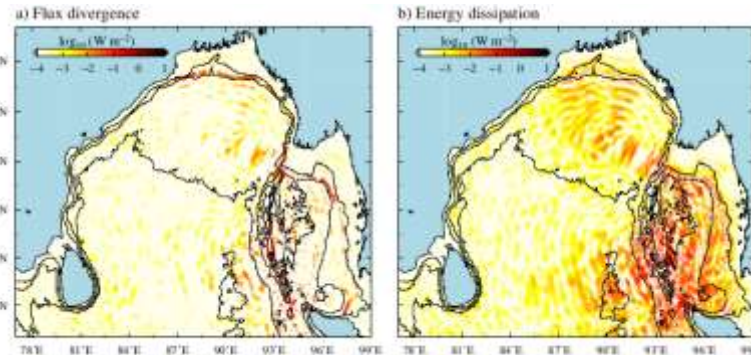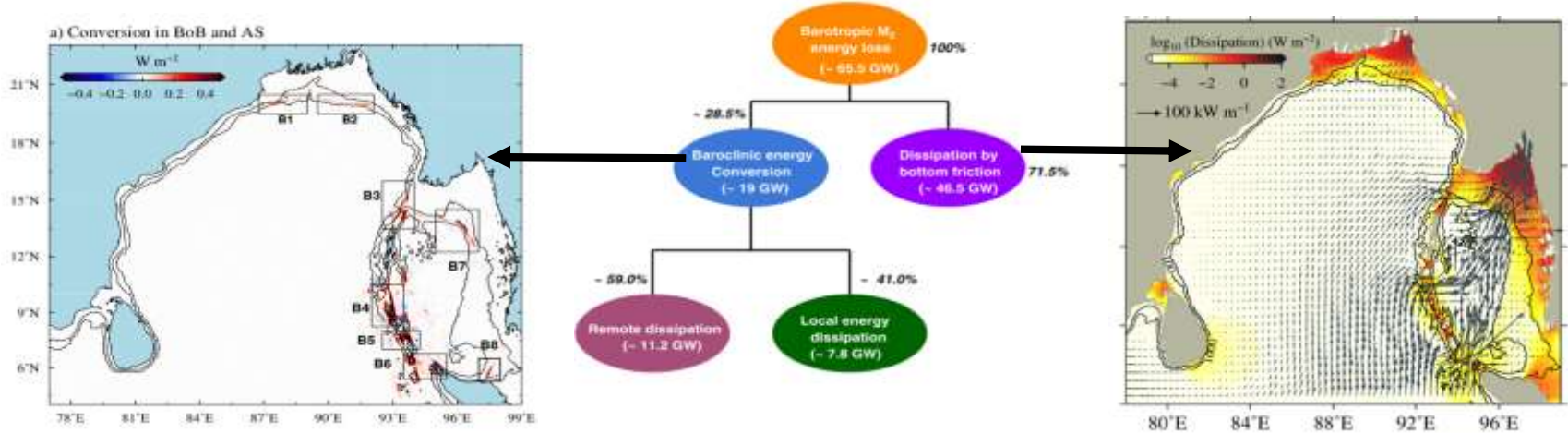
Strong Dissipation in the Andaman Sea

a) Flux divergence

b) Energy dissipation

4) Spring-neap variability of conversion and flux in the Bay of Bengal and Andaman Sea

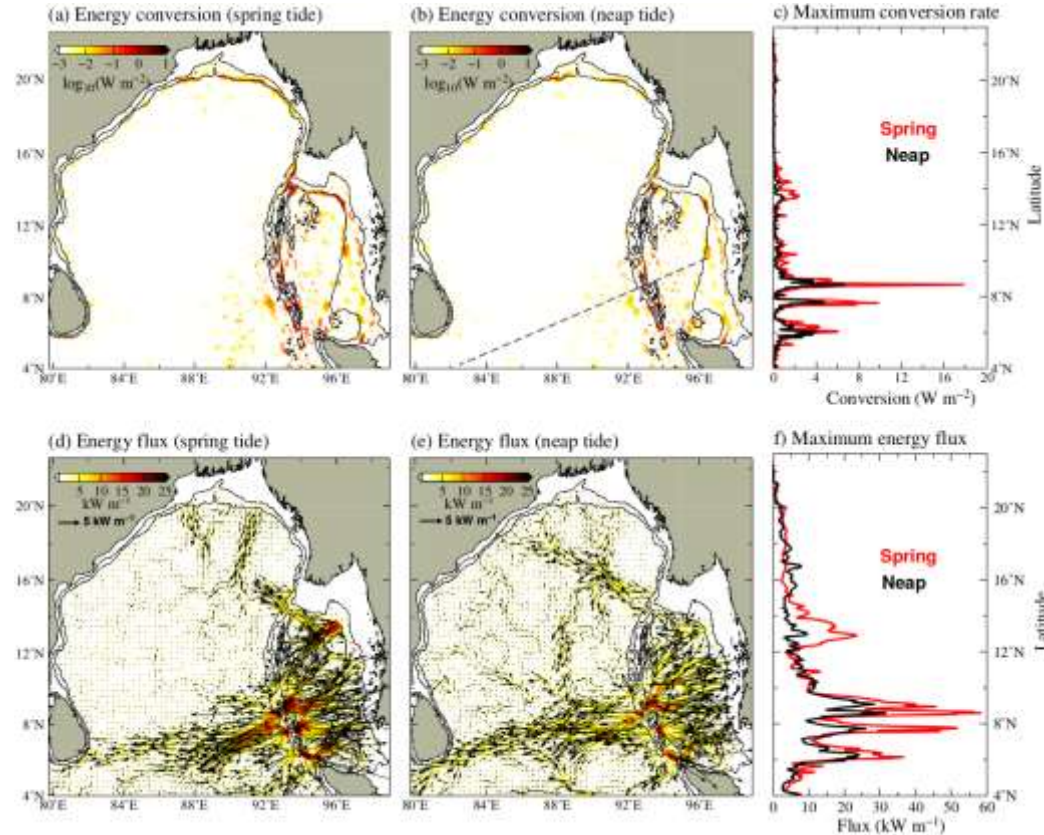- **About 60% change in energy conversion**

- **Energy conversion**
 **27.0 GW (spring)**
  11.02 GW (neap)

- **Along the AN Ridge,**
  21.45 GW (spring)
  8.65 GW (neap)

(a) Energy conversion (spring tide)
(b) Energy conversion (neap tide)
c) Maximum conversion rate
(d) Energy flux (spring tide)
(e) Energy flux (neap tide)
f) Maximum energy flux

5) Effect of mesoscale circulation on the propagation of internal tides

- **The variations in the path of internal tide propagation due to mesoscale circulation.**

- **This causes large intraseasonal variability in internal tide activity along the continental margins of the western BoB.**
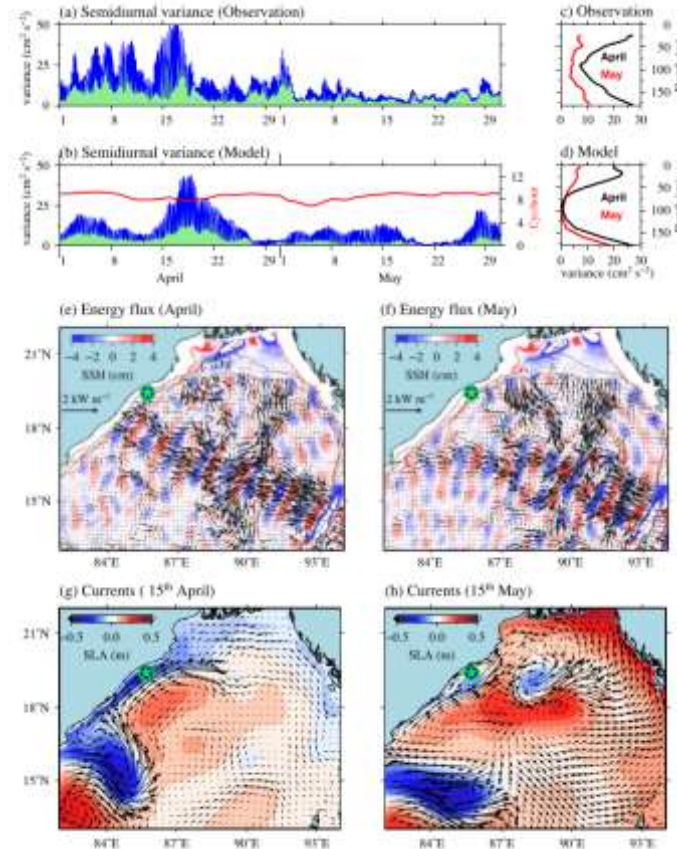
Summary

Barotropic tides :

Basics

Modelling

Satellite observations

Internal tides

Modelling

Satellite observations

Energy budget

Reference

https://www.education.com/science-fair/article/barycenter-balancing-point/

https://beltoforion.de/en/tides/tidal_cycles.php

All Web sources

Thank You….